VOL. 291 NO. 11 NOVEMBER 2008

The Anatomical Record

Advances in Integrative Anatomy and Evolutionary Biology

The Paranasal Sinuses: The Last Frontier in Craniofacial Biology

Celebrating OVER 100 YEARS *of Excellence in* ANATOMICAL PUBLICATION

THE ANATOMICAL RECORD NOVEMBER 2008 VOL. 291-NO. 11-PAGES 1343-1572 WILEY-BLACKWELL
AN OFFICIAL PUBLICATION OF THE AMERICAN ASSOCIATION OF ANATOMISTS KURT H. ALBERTINE • EDITOR-IN-CHIEF

THE ANATOMICAL RECORD 291:1362–1388 (2008)

The Paranasal Air Sinuses of Predatory and Armored Dinosaurs (Archosauria: Theropoda and Ankylosauria) and Their Contribution to Cephalic Structure

LAWRENCE M. WITMER* AND RYAN C. RIDGELY
Department of Biomedical Sciences, College of Osteopathic Medicine,
Ohio University, Athens, Ohio

ABSTRACT

The paranasal air sinuses and nasal cavities were studied along with other cephalic spaces (brain cavity, paratympanic sinuses) in certain dinosaurs via CT scanning and 3D visualization to document the anatomy and examine the contribution of the sinuses to the morphological organization of the head as a whole. Two representatives each of two dinosaur clades are compared: the theropod saurischians *Majungasaurus* and *Tyrannosaurus* and the ankylosaurian ornithischians *Panoplosaurus* and *Euoplocephalus*. Their extant archosaurian outgroups, birds and crocodilians (exemplified by ostrich and alligator), display a diversity of paranasal sinuses, yet they share only a single homologous antorbital sinus, which in birds has an important subsidiary diverticulum, the suborbital sinus. Both of the theropods had a large antorbital sinus that pneumatized

Anatomical abbreviations used (taxonomic representation indicated in parentheses): airway = main nasal airway (respiratory region of the nasal cavity; all); antorb = antorbital sinus (archosaurs); aofen = internal antorbital fenestra in the skull; the external antorbital fenestra is the rim around the antorbital fossa (*Majungasaurus*, *Tyrannosaurus*); caudal loop = caudal loop of the nasal airway (*Panoplosaurus*, *Euoplocephalus*); ch = choana (all); dalv = dorsal alveolar canal, transmitting branches of the maxillary nerves and large vessels (*Euoplocephalus*); con = conchal spaces in the airway of the ostrich, where the mucosal nasal conchae reside; ect = ectopterygoid sinus (source of diverticulum uncertain, probably not from antorbital sinus; *Tyrannosaurus*); endocast = cranial endocast of brain cavity (all); eth = ethmoidal sinus (human); fr = frontal sinus (human; in ostrich, frontal portion of fronto-ethmoidal sinus; *Majungasaurus*); ialv = interalveolar sinuses (a maxillary sinus, from antorbital sinus via other maxillary sinuses; *Tyrannosaurus*); jug = jugal sinus (from antorbital sinus; *Tyrannosaurus*); lac = lacrimal sinus proper (from antorbital sinus in nonavian theropods including most birds but from suborbital sinus in ostrich); lacm = medial lacrimal sinus (from antorbital sinus in nonavian theropods); mant = maxillary antral sinus (a maxillary sinus, from antorbital sinus; *Tyrannosaurus*); max = maxillary sinus (human, alligator, theropods—nonhomologous); mes = mesethmoidal portion of fronto-ethmoidal sinus (ostrich); mfen = maxillary fenestra of skull (*Tyrannosaurus*); mnas = medial nasal canal, transmitting the medial nasal branches of the ophthalmic nerve and enlarged medial nasal branches of the ethmoidal vessels (*Euoplocephalus*); nar = nostril (fossil skulls); nas = nasal sinus (from antorbital sinus; *Majungasaurus*); npdu = nasopharyngeal duct (alligator); nvas = neurovascular canals in the premaxilla derived principally from the medial nasal canal (*Euoplocephalus*); olf = olfactory region of the nasal cavity (all); orbit = orbit or eye socket (fossil skulls); pf = prefrontal sinus (alligator); pal = palatine sinus (alligator, *Tyrannosaurus*, *Panoplosaurus, Euoplocephalus*—not homologous); pmax = promaxillary sinus (a maxillary sinus, from antorbital sinus; *Tyrannosaurus*); pter = pterygoid sinus (from nasopharyngeal duct in alligator, from suborbital sinus in ostrich); pterpal = pterygopalatine sinus of nasopharyngeal duct (alligator); pv = postvestibular sinus (alligator); rostral loop = rostral loop of the nasal airway (*Panoplosaurus*, *Euoplocephalus*); sph = sphenoidal sinus (human); squ = squamosal sinus (perhaps from antorbital sinus via suborbital sinus; *Tyrannosaurus*); sub = suborbital sinus (from antorbital sinus in theropods, including ostrich); tymp = main middle ear cavity and paratympanic sinuses (all); * = position of the putative "paranasal aperture," which is not demonstrably separate either externally or internally from the true narial aperture (*Euoplocephalus*).

Grant sponsor: National Science Foundation; Grant numbers: NSF BSR-9112070, NSF IBN-9601174, NSF IBN-0343744, NSF IOB-0517257; Grant sponsor: Ohio University College of Osteopathic Medicine.

*Correspondence to: Lawrence M. Witmer, Department of Biomedical Sciences, College of Osteopathic Medicine, Ohio University, Athens, OH 45701. Fax: 740-593-2400.
E-mail: witmerL@ohio.edu

Received 22 April 2008; Accepted 23 April 2008
DOI 10.1002/ar.20794
Published online in Wiley InterScience (www.interscience.wiley.com).

many of the facial and palatal bones as well as a birdlike suborbital sinus. Given that the suborbital sinus interleaves with jaw muscles, the paranasal sinuses of at least some theropods (including birds) were actively ventilated rather than being dead-air spaces. Although many ankylosaurians have been thought to have had extensive paranasal sinuses, most of the snout is instead (and surprisingly) often occupied by a highly convoluted airway. Digital segmentation, coupled with 3D visualization and analysis, allows the positions of the sinuses to be viewed in place within both the skull and the head and then measured volumetrically. These quantitative data allow the first reliable estimates of dinosaur head mass and an assessment of the potential savings in mass afforded by the sinuses. Anat Rec, 291:1362–1388, 2008.

Key words: dinosaur; theropod; ankylosaur; bird; crocodilian; human; paranasal sinus; computed tomography; gross anatomy

Paranasal air sinuses are seemingly ubiquitous features of mammals, and studies of mammalian paranasal sinuses—particularly those of humans (Fig. 1) and other primates—are diverse in both taxonomic and biological scope, impacting debates pertaining to systematics, biomechanics, physiology, development, medicine, and paleontology, among others (e.g., see articles in this issue and in Koppe et al., 1999). Mammals are not alone, however, in having air-filled epithelial diverticula of the nasal cavity that pneumatize the facial skeleton. Archosaurs are another highly pneumatic clade. Archosauria is the sauropsid clade comprised of birds and crocodilians today, and including such extinct Mesozoic forms as nonavian dinosaurs, pterosaurs, and a variety of basal taxa. The paranasal sinuses of mammals and archosaurs are not homologous (Witmer, 1995b), and, although various extracapsular epithelial diverticula have been described for different tetrapod groups (e.g., amphibians, squamate reptiles), only mammals and archosaurs display pneumatic invasion of the bones of the face and cranium (Witmer, 1999). In archosaurs, pneumatic diverticula may arise from all parts of the nasal cavity, including the nasal vestibule (e.g., some hadrosaurid and ankylosaurid dinosaurs) and nasopharyngeal duct (e.g., crocodilians), but, as in mammals, the nasal cavity proper (cavum nasi proprium) is the source of the major paranasal air sinus, called the antorbital sinus because it is lodged within the bony antorbital cavity (Witmer, 1990, 1995b, 1997a,b, 1999; Hill et al., 2003).

Archosaurian and mammalian paranasal sinuses are quite different from each other in that, whereas mammalian sinuses (Fig. 1) tend to be almost fully enclosed within bone (connected by typically narrow ostia), archosaur sinuses tend to be much more open and less constrained. The archosaurian antorbital sinus is usually partially enclosed within the lacrimal bone caudally and maxilla rostrally and variably floored by the palatine bone and roofed by the nasal bone. The antorbital sinus itself has subsidiary diverticula that invade and pneumatize many of the surrounding bones, although such accessory cavities are best developed in theropod dinosaurs, including birds (see Witmer, 1997a,b). In most taxa the antorbital sinus is exposed laterally, being covered only by skin. Moreover, in birds the antorbital sinus has a subsidiary diverticulum (the suborbital or "infraorbital" sinus) that extends caudally from the antorbital cavity into the orbit where it is juxtaposed between the eyeball, jaw muscles, and other structures (Bang and Wenzel, 1985; Witmer, 1990, 1995b; Evans, 1996). New evidence suggests that such a suborbital sinus is found in at least the theropodan ancestors of birds, if not even more broadly among archosaurs (Witmer, 1997a; Sampson and Witmer, 2007). Thus, the paranasal sinuses of most archosaurs are not the familiar blind sacs housed within bony chambers of mammals but rather are more expansive and relate directly to (i.e., contact) a diversity of other anatomical systems.

This article seeks to explore not just the morphology of select dinosaur paranasal air sinuses but also the relationship to other anatomical systems, such as the airway, the olfactory chamber of the nasal cavity, the paratympanic air sinuses, the orbital contents, and the brain and endocranial cavity, among others. Examining the contribution of the paranasal sinuses to the architecture of the head as a whole is now possible, thanks to the development of computed tomography (CT scanning) coupled with 3D computer visualization. These new approaches allow many different anatomical structures of extinct and extant animals alike to be viewed in place within the skull or head, as well as to be analyzed quantitatively. The power of 3D visualization will be used to illustrate the anatomy rather than lengthy morphological description. After looking briefly at the sinuses of the modern relatives of dinosaurs, the focus will turn to two predatory dinosaurs with which the authors have extensive experience and on which they have published previously: the Cretaceous abelisaurid theropod from Madagascar, *Majungasaurus crenatissimus* (Witmer et al., 2004; Sampson and Witmer, 2007), and the Cretaceous coelurosaur *Tyrannosaurus rex* from North America (Witmer, 1997a; Witmer and Ridgely, 2005; Witmer et al., 2008). These two theropods allow a look at a dinosaur system in which paranasal pneumaticity is relatively well understood, and which can be integrated into a more comprehensive picture of cephalic anatomy. Two North American Cretaceous armored ankylosaurian dinosaurs also will be investigated: the nodosaurid *Panoplosaurus mirus* and the ankylosaurid *Euoplocephalus tutus*. These provide the opportunity to investigate a classically problematic nasal and

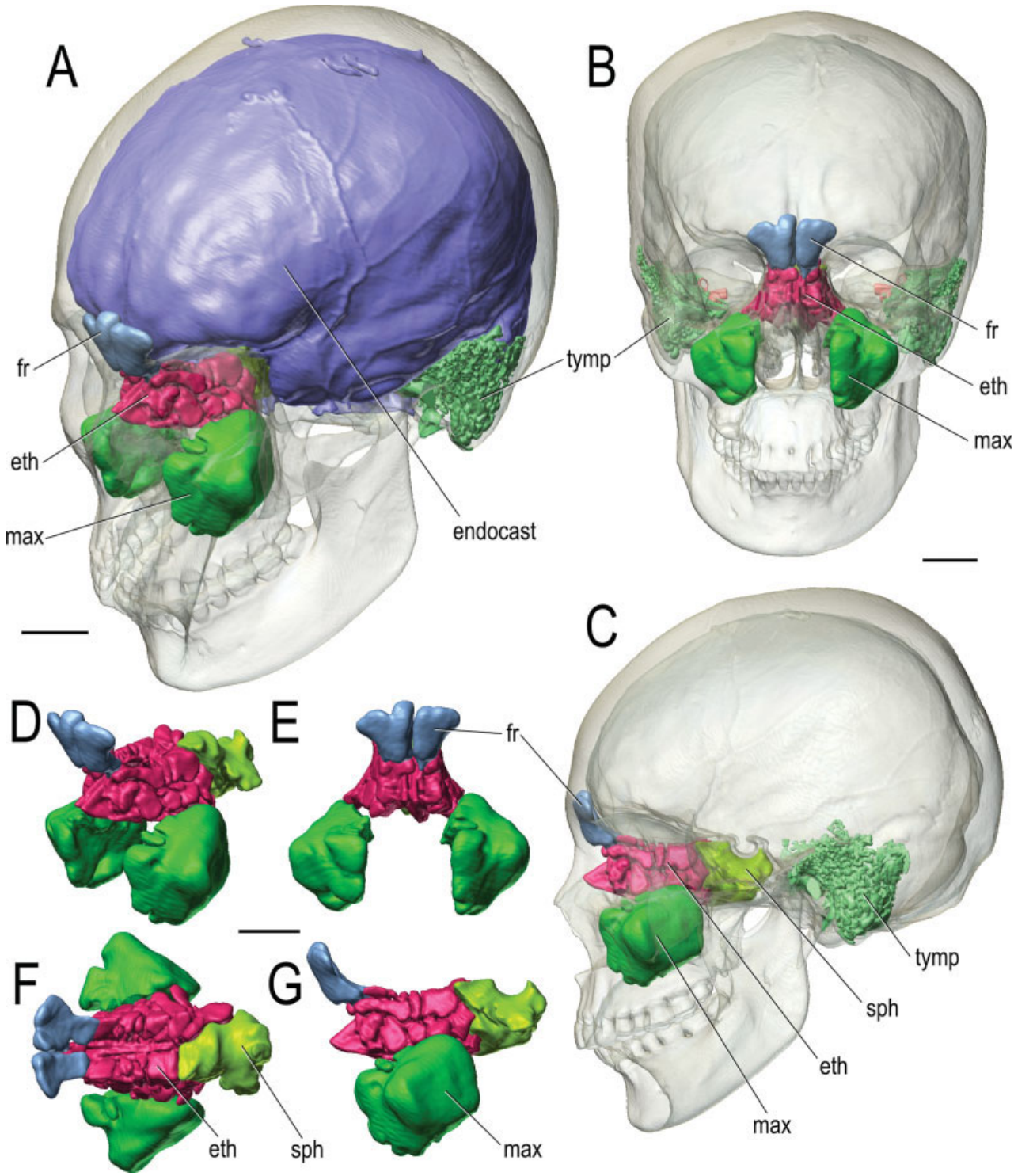

Fig. 1. Paranasal sinuses and other cephalic components of a human (*Homo sapiens*, OUVC 10503) based on CT scanning followed by segmentation and 3D visualization. Bone is rendered semitransparent. **A:** Left anterodorsolateral view. **B:** Anterior view. **C:** Left lateral view. **D–G:** isolated paranasal sinuses. D: Left anterodorsolateral view corresponding to A. E: Anterior view corresponding to B. F: Dorsal view. G: Left lateral view corresponding to C. The paratympanic sinuses and endosseous labyrinth are also visualized. Scale bars = 2 cm.

paranasal sinus system, and, it is hoped, shed some new light, although as will be seen, these armored dinosaurs have truly bizarre systems. Finally, the new analytical capabilities provided by CT scanning will be used to calculate volumes and masses for cephalic structures in the two theropods, providing not only the first reliable estimates of head mass but also an assessment of the impact of the paranasal sinuses on head mass.

MATERIALS AND METHODS

Materials

The dinosaur sample largely focuses on four main taxa. (1) Archosauria, Dinosauria, Theropoda, Abelisauridae, *Majungasaurus crenatissimus*; Field Museum of Natural History (FMNH, Chicago) PR2100; collected from the Upper Cretaceous (Maastrichtian, 66–71 Ma) Maevarano Formation of northwestern Madagascar (Krause et al., 2007). (2) Archosauria, Dinosauria, Theropoda, Coelurosauria, Tyrannosauridae, *Tyrannosaurus rex*; FMNH PR2081 (as well as a restored, one-third-scale sculpture of FMNH PR2081 crafted by Brian Cooley), American Museum of Natural History (AMNH, New York City) FR 5117, Black Hills Institute (BHI, Hill City, SD) 3033, and an unnumbered Carnegie Museum of Natural History (Pittsburgh) skull; collected from the Upper Cretaceous (Maastrichtian, 66–71 Ma) Hell Creek and Lance Formations of Montana, Wyoming, and South Dakota. (3) Archosauria, Dinosauria, Ornithischia, Ankylosauria, Nodosauridae, *Panoplosaurus mirus*; Royal Ontario Museum (ROM, Toronto) 1215 [note: referral to *P. mirus* follows Coombs (1978), Carpenter (1990), and Vickaryous et al. (2004), although Russell (1940) and Ryan and Evans (2005) referred it to *Edmontonia rugosidens*]; collected from the Upper Cretaceous (Campanian, 83–71 Ma) Dinosaur Park Formation of Alberta. (4) Archosauria, Dinosauria, Ornithischia, Ankylosauria, Ankylosauridae, *Euoplocephalus tutus*; AMNH FR 5405; collected from the Upper Cretaceous (Campanian, 83–71 Ma) Dinosaur Park Formation of Alberta. Two additional ankylosaur specimens became available late enough in the study that it was not possible to perform the same level of analysis and visualization, although important details were assessed. One specimen is another skull of *E. tutus* (AMNH FR 5403), and the other is a skull of *Edmontonia rugosidens* (AMNH FR 5381), a nodosaurid closely related to *Panoplosaurus*. As with the other ankylosaurs in the sample, these specimens derive from the Dinosaur Park Formation of Alberta.

Inferences about the unpreserved traits of extinct dinosaur taxa are grounded in the extant phylogenetic bracket approach (Witmer, 1995a) whereby extant outgroups (in this case, birds and crocodilians) provide critical data on soft tissues and their osteological correlates. Although numerous extant birds and crocodilians were examined, data are presented here on a characteristic representative of each. (1) Archosauria, Suchia, Crocodylia, Alligatoridae, *Alligator mississippiensis* (American alligator); Ohio University Vertebrate Collections (OUVC) 9761; fresh carcass of adult (total skull length: 371 mm) obtained from the Rockefeller Wildlife Refuge, Grand Chenier, Louisiana. (2) Archosauria, Dinosauria, Theropoda, Aves, Ratitae, *Struthio camelus* (ostrich); OUVC 10491; fresh head and neck of adult (total skull length: 182 mm) purchased from a commercial source. For further comparison and illustration, a human skull (*Homo sapiens*, OUVC 10503) was also analyzed. Figure 2 presents the phylogenetic relationships of the taxa mentioned in this article.

Reference was also made to an existing series of avian specimens in which the paranasal sinuses were injected with latex followed by removal of soft tissue (for methods, see Witmer, 1995b). These skull-sinus preparations included the following specimens: juvenile (6 weeks old) ostrich, *Struthio camelus* (OUVC 10504); six adult domestic chicken, *Gallus gallus* (OUVC 10259–10264); one hatchling (OUVC 10254) and two adult (OUVC 10257–10258) domestic goose, *Anser anser*; four adult domestic ducks, *Anas platyrhynchos* (OUVC 10248–10251); and one adult ring-billed gull, *Larus delawarensis* (OUVC 10308).

CT Scanning and 3D Visualization

Other than the latex-injected specimens, all of the above, both extant and extinct, were subjected to CT scanning at O'Bleness Memorial Hospital, Athens, Ohio, using a General Electric (GE) LightSpeed Ultra Multislice CT scanner equipped with the Extended Hounsfield option (which greatly improves resolvability of detail from dense objects such as fossils by extending the dynamic range of images as much 16-fold) and a "bowtie" filter (which decreases beam-hardening artifacts). All specimens were scanned helically at a slice thickness of 625 μm, 120–140 kV, and 200–300 mA. The raw scan data were reconstructed using a bone algorithm. Data were output from the scanners in DICOM format, and then imported into Amira 3.1.1 or 4.1.2 (Mercury-TGS, Chelmsford, MA) for viewing, analysis, and visualization. The only exceptions to the above protocol were FMNH PR2081 (scanned elsewhere; see Brochu, 2003), the Carnegie Museum *Tyrannosaurus* (scanned at NASA's Marshall Space Flight Center in Alabama), and BHI 3033. All CT data, regardless of source, were analyzed on 32- and 64-bit PC workstations with 4 GB of RAM and nVidia Quadro FX 3000 or 4500 video cards and running Microsoft Windows XP Professional, Windows XP Professional x64, or Linux 2.6.18 (Debian 4.0 distribution). Structures of interest (e.g., paranasal sinuses, cranial endocast, otic labyrinth, paratympanic sinuses, etc.) were highlighted and digitally extracted using Amira's segmentation tools for quantification and visualization.

The theropod studies each require additional explanation. As described in Sampson and Witmer (2007), the skull of *Majungasaurus* used here (FMNH PR2100) was discovered as largely disarticulated bony elements. Many of the individual fossil elements were CT scanned, as was a cast of the full skull, which had been assembled from the individual cast elements. In Amira, the CT datasets from the fossil elements were then registered (aligned) to the dataset of the skull cast, which thus allowed the sinuses segmented from the fossil elements to be "plugged into" their proper places in the full skull. As noted above, not all air sinuses in archosaurs are fully enclosed in bone, and thus the skull and structures segmented in Amira were imported into the 3D modeling software Maya 8.5 (Autodesk, San Rafael, CA) to model the antorbital sinus and its suborbital diverticulum,

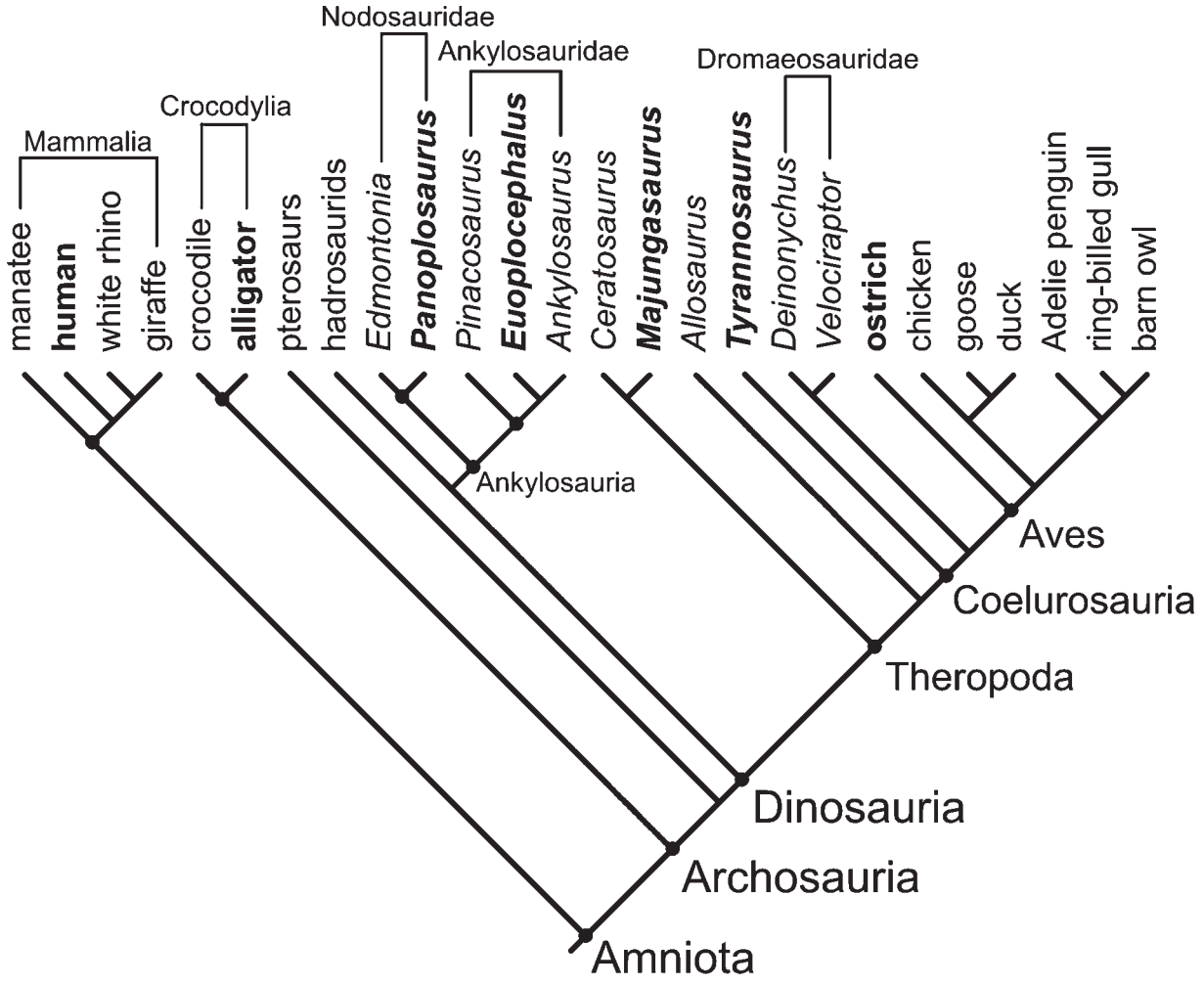

Fig. 2. Diagram of phylogenetic relationships of the taxa mentioned in the text. The focal taxa are indicated in boldface type. Topology derives from Hill et al. (2003), Holtz et al. (2004), Vickaryous et al. (2004), Bininda-Emonds et al. (2007), and Livezey and Zusi (2007).

as well as the middle ear sac (based on a series of anatomical criteria that will be presented elsewhere). A similar approach was used for *Tyrannosaurus*, although, whereas the *Majungasaurus* system represents a single specimen, the *Tyrannosaurus* system represents a composite based on structures segmented or modeled from multiple specimens and then all digitally inserted into the restored sculpture.

Supplemental visualizations as well as the native CT data for some of the specimens are available on the authors' website: www.ohio.edu/witmerlab.

Mass Estimation of Theropod Dinosaur Heads

Novel data on mass of the fleshed-out heads in the two theropods in the sample are presented here. These were calculated by generating volumes for various cephalic components from the CT data and then converting these volumes to masses. More specifically, the skull models were digitally "wrapped" with a skin, taking into account jaw muscle bulges (from Holliday, 2006) but ignoring the cervicocephalic musculature; total head volume was calculated from this skin surface. The head was modeled with the jaws completely adducted such that the oral cavity is a potential (not a real) space, which is appropriate based on the authors' findings from CT data of a broad diversity of extant amniotes. Skull volume was generated directly from the CT scans of the *Majungasaurus* and *Tyrannosaurus* skull casts (see above); for *Majungasaurus*, the vomer and right pterygoid were digitally reconstructed, and this volume was added to the total. Based on digital segmentation, the volumes of all of the paranasal and paratympanic sinuses, as well as of the cranial endocast (brain cavity) were calculated, and these were then subtracted from the skull cast volumes to get a very realistic volume for the bone comprising the skull. In truth, these bone volumes are very slight overestimates, because it was not possible to consider the minute intertrabecular spaces and tiny neurovascular canals within the bone; this source of error is regarded as negligible and probably within measurement error and natural individual

TABLE 1. Volumes, tissue densities, and masses for head structural components and the head itself of *Majungasaurus crenatissimus* under three different states of pneumaticity

		Head with all pneumatic sinuses		Head without paranasal sinuses[a]		Head without paranasal or paratympanic sinuses[a]	
	Volume (cm^3)	Density (g/cm^3)	Mass (g)	Density (g/cm^3)	Mass (g)	Density (g/cm^3)	Mass (g)
Bone[b]	5909.5	1.35	7977.8	1.35	7977.8	1.35	7977.8
Cranial endocast	126.2	1.036	130.7	1.036	130.7	1.036	130.7
Nasal cavity							
Airway	643.7	0.0	0.0	0.0	0.0	0.0	0.0
Olfactory region	1230.3	0.0	0.0	0.0	0.0	0.0	0.0
Paranasal sinuses							
Antorbital sinus	777.8	0.0	0.0	1.35	1050.0	1.35	1050
Maxillary sinus	5.3	0.0	0.0	1.35	7.2	1.35	7.2
Lacrimal sinus proper	37.2	0.0	0.0	1.35	50.2	1.35	50.2
Medial lacrimal sinus	9.0	0.0	0.0	1.35	12.2	1.35	12.2
Nasal sinus	429.2	0.0	0.0	1.35	579.4	1.35	579.4
Frontal sinus	86.1	0.0	0.0	1.35	116.2	1.35	116.2
Suborbital sinus	403.3	0.0	0.0	1.05	423.5	1.05	423.5
Middle ear cavity	716.4	0.0	0.0	0.0	0.0	0.0	0.0
Paratympanic sinuses	29.5	0.0	0.0	0.0	0.0	1.35	39.8
Soft tissue	22850.8	1.05	23993.3	1.05	23993.3	1.05	23993.3
Total head[a]	33254.3	–	32101.8	–	34340.5	–	34380.3
Skull mass[a]	–	–	7977.8	–	9793.0	–	9832.8

[a]For the calculations of head mass and skull mass in the absence of pneumatic sinuses, the various sinus cavities are assigned the density of bone.
[b]Includes restored vomer and right pterygoid.

variation, but it does represent a target for future refinements in technique. The form of the suborbital sinus, which is not enclosed in bone (see below), was modeled in Amira and Maya based on anatomical landmarks in the fossils and the structure of the sinus in birds. Subtracting the volumes of the bony skull, air sinuses, and endocast from total head volume gives the volume of the remaining soft tissue.

To convert volumes to masses, volume (cm^3) was multiplied by density (g/cm^3). Ignoring the thin sinus epithelium, air sinus density was taken as zero, as was the resulting mass. Density of the cranial endocast was assigned the density of brain tissue, using the commonly used 1.036 g/cm^3 value (e.g., Witmer et al., 2003). The soft-tissue volume in life included a heterogeneous mix of muscle, fat, nerves, vessels, and so forth, but muscle certainly predominated. Common literature values for muscle density (e.g., Urbanchek et al., 2001) are 1.06 g/cm^3, and thus, for the "soft-tissue" density value used here, that muscle value was arbitrarily reduced to 1.05 g/cm^3 to account for fat and other tissue types. The bone density values in the literature are somewhat unsatisfactory in that they tend to be derived from small cubes of mammalian bone of particular types (e.g., compact, trabecular, otic), whereas skulls include virtually all bone types as well as teeth. Consequently, whole-skull density values were generated for a range of avian, crocodilian, and mammalian skulls by dividing the mass of the skull (as weighed on a digital balance) by the volume of the skull (as determined by CT scanning to be consistent with the fossil sample). The resulting bone density values ranged from 0.5 g/cm^3 (barn owl, *Tyto alba*) to 1.7 g/cm^3 (Adelie penguin, *Pygoscelis adeliae*), with a total sample mean of 1.2 g/cm^3. However, the avian sample was excluded because birds lack teeth, and consequently the mean of the remaining sample (1.35 g/cm^3) was used. This value is still somewhat lower than typical values for bone density in the literature (e.g., Currey, 1984), suggesting that whole skulls have relatively lower densities than bone explants from the appendicular skeleton. For example, Yang et al. (2002, p 313) reported "normal human bone density" as 1.85 g/cm^3, yet the whole-skull density calculated here for humans was 1.1 g/cm^3.

In addition to simply estimating head mass, the contribution of pneumaticity to total head mass (thus assessing any weight savings) was estimated by doing calculations in which the paranasal sinuses were considered to be bone by assigning the sinus volumes the density of bone (except for the suborbital sinus which was assigned the density of soft tissue). Similar calculations considering the head to be completely without any pneumatic sinuses (yet retaining the main nasal and middle ear cavities) were made by assigning bone density to the paratympanic as well as the paranasal sinuses. For comparison, similar calculations were also made for the human skull in the sample. The volumes and masses of all relevant structures for *Majungasaurus*, *Tyrannosaurus*, and *Homo sapiens* are presented in Tables 1–3, respectively.

RESULTS AND OBSERVATIONS

The Modern Archosaurian Condition: Alligator and Ostrich

The extant relatives of dinosaurs are particularly relevant, not only because they can be directly examined (e.g., via dissection, medical imaging) for the detailed relationships between the soft tissues and the skeleton, but also because, being close phylogenetic relatives, their attributes have a greater likelihood of being homologous to those of dinosaurs (Witmer, 1995a). For example, the bony antorbital cavities of extant birds and

TABLE 2. Volumes, tissue densities, and masses for head structural components and the head itself of *Tyrannosaurus rex* under three different states of pneumaticity

		Head with all pneumatic sinuses		Head without paranasal sinuses[a]		Head without paranasal or paratympanic sinuses[a]	
	Volume (cm^3)	Density (g/cm^3)	Mass (g)	Density (g/cm^3)	Mass (g)	Density (g/cm^3)	Mass (g)
Bone	122709.8	1.35	165658.2	1.35	165658.2	1.35	165658.2
Cranial endocast[b]	1174.9	1.036	1217.2	1.036	1217.2	1.036	1217.2
Nasal cavity							
Airway[c]	10740.0	0.0	0.0	0.0	0.0	0.0	0.0
Olfactory region[c]	19057.8	0.0	0.0	0.0	0.0	0.0	0.0
Paranasal sinuses							
Antorbital sinus[c]	6766.1	0.0	0.0	1.35	9134.2	1.35	9134.2
Maxillary sinuses[d]	7772.5	0.0	0.0	1.35	10492.9	1.35	10492.9
Lacrimal sinus proper[e]	1177.1	0.0	0.0	1.35	1589.1	1.35	1589.1
Medial lacrimal sinus[e]	136.2	0.0	0.0	1.35	183.9	1.35	183.9
Jugal sinus[f]	1031.3	0.0	0.0	1.35	1392.2	1.35	1392.2
Palatine sinus[c]	1082.5	0.0	0.0	1.35	1461.4	1.35	1461.4
Squamosal sinus[f]	1377.4	0.0	0.0	1.35	1859.5	1.35	1859.5
Suborbital sinus[c]	9710.6	0.0	0.0	1.05	10196.1	1.05	10196.1
Middle ear cavity[c]	13791.3	0.0	0.0	0.0	0.0	0.0	0.0
Paratympanic sinuses							
Braincase sinuses[b]	2254.3	0.0	0.0	0.0	0.0	1.35	3043.3
Quadrate sinus[e]	482.1	0.0	0.0	0.0	0.0	1.35	650.8
Articular sinus[f]	743.2	0.0	0.0	0.0	0.0	1.35	1003.3
Ectopterygoid sinus[e]	1641.3	0.0	0.0	0.0	0.0	1.35	2215.8
Soft tissue	332050.1	1.05	348652.6	1.05	348652.6	1.05	348652.6
Total head[a]	533698.5	–	515528.0	–	551837.3	–	558750.5
Skull mass[a]	–	–	165658.2	–	191771.4	–	198684.6

[a]For the calculations of head mass and skull mass in the absence of pneumatic sinuses, the various sinus cavities are assigned the density of bone.
[b]Segmented from AMNH 5117.
[c]Restored one-third scale sculpture of FMNH PR2081.
[d]Segmented from BHI 3033; includes promaxillary recess, maxillary antrum, and interalveolar recesses.
[e]Segmented from Carnegie museum skull.
[f]Segmented from FMNH PR2081.

TABLE 3. Volumes, tissue densities, and masses for head structural components and the head itself of *Homo sapiens* under three different states of pneumaticity

		Head with all pneumatic sinuses		Head without paranasal sinuses[a]		Head without paranasal or paratympanic sinuses[a]	
	Volume (cm^3)	Density (g/cm^3)	Mass (g)	Density (g/cm^3)	Mass (g)	Density (g/cm^3)	Mass (g)
Bone	577.3	1.1[b]	635.0	1.1[b]	635.0	1.1[b]	635.0
Cranial endocast	1178.7	1.036	1221.1	1.036	1221.1	1.036	1221.1
Nasal cavity	45.1	0.0	0.0	0.0	0.0	0.0	0.0
Paranasal sinuses							
Maxillary sinus	29.5	0.0	0.0	1.1[b]	32.4	1.1[b]	32.4
Frontal sinus	3.2	0.0	0.0	1.1[b]	3.5	1.1[b]	3.5
Sphenoid sinus	8.7	0.0	0.0	1.1[b]	9.6	1.1[b]	9.6
Ethmoidal sinuses	7.1	0.0	0.0	1.1[b]	7.8	1.1[b]	7.8
Middle ear cavity	0.4	0.0	0.0	0.0	0.0	0.0	0.0
Paratympanic sinuses	11.5	0.0	0.0	0.0	0.0	1.1[b]	12.6
Soft tissue	739.3	1.05	776.3	1.05	776.3	1.05	776.3
Total head[a]	2600.8	–	2632.4	–	2685.7	–	2698.3
Skull mass[a]	–	–	635.0	–	688.3	–	700.9

[a]For the calculations of head mass and skull mass in the absence of pneumatic sinuses, the various sinus cavities are assigned the density of bone.
[b]Bone density for this specimen of *H. sapiens* (OUVC 10503) was determined empirically from this specimen itself, and so this value is used rather than the estimate generated from a larger, more diverse sample used for the dinosaurs.

crocodilians—despite dramatic differences stemming from over 230 million years of divergent evolution—house a homologous paranasal air sinus (the antorbital sinus), suggesting that the antorbital cavity of dinosaurs likewise housed the same homologous antorbital air sinus (Witmer, 1997a). Nevertheless, long divergent evolution of the clades leading to modern birds and crocodilians has produced significant differences. The structure

of the paranasal sinuses in extant archosaurs has been described in detail previously (see Witmer, 1990, 1995b, 1999; and references therein), and will only be summarized here, although the opportunity is taken to provide new visualizations (Figs. 3 and 4) that also demonstrate the relationship of the paranasal sinuses to other anatomical systems (e.g., brain cavity, tympanic cavity and its sinuses).

Alligator mississippiensis (e.g., OUVC 9761) is a good representative of the extant crocodilian condition (Fig. 3), although different species have somewhat different sinuses (Wegner, 1958; Witmer, 1995b). Perhaps the most remarkable attribute of extant crocodilian paranasal sinuses is that the antorbital sinus (the "caviconchal sinus" of the old literature) is enclosed laterally within bone; that is, the antorbital fenestra, the most quintessentially archosaurian character, is apomorphically lost, both ontogenetically (Witmer, 1995b) and phylogenetically (Witmer, 1997a). The antorbital sinus, however, remains, and in some ways it is much like the mammalian maxillary sinus in being largely enclosed within the maxillary bone. The antorbital sinus in large alligators (such as OUVC 9761) has a medial diverticulum inflating the palatal process of the maxilla (Fig. 3). Crocodilians have a range of other paranasal sinuses arising from the nasal cavity proper, such as, in alligators, the postvestibular sinus and the prefrontal sinus (Fig. 3). The nasal airway is very long in crocodilians, owing largely to their extensive secondary palate. The airway enters the long nasopharyngeal duct, formed by the vomers, palatines, and pterygoids, on its way to the pharynx where it opens at the secondary choana. Along the way, the nasopharyngeal duct gives rise to several paranasal sinuses, such as in large alligators, the vomerine bullar sinus, the pterygopalatine bullar sinus, and the pterygoid sinus (for illustration of other such sinuses, see Wegner, 1958; Witmer, 1995b, 1999). Paranasal sinuses arising from the nasopharyngeal duct appear to be restricted to the lineage leading to crocodilians and are absent in mammals (Witmer, 1999; and references therein).

Birds are particularly relevant to the issue of dinosaur paranasal sinuses, because birds are themselves evolutionarily nested within the clade of theropod dinosaurs—that is, birds are dinosaurs. As basal, large-bodied modern birds, ratites such as ostriches (*Struthio camelus*, OUVC 10491; Fig. 4) are potentially good models for nonavian theropods (and, as it turns out, ostriches are fairly typical for birds with regard to paranasal sinuses). Birds share only a single paranasal sinus with crocodilians, the antorbital sinus, which is, in fact, the only paranasal air sinus that can be homologized across Archosauria (Witmer, 1997a). In comparison with most archosaur groups, the avian antorbital cavity (and hence the sinus within) is relatively small in volume, largely as a result of expansion of the nasal vestibule and eyeball, which together compress the paranasal space (Witmer, 1995b). Nevertheless, through its many diverticula (Witmer, 1990), the antorbital sinus pneumatizes much of the surrounding skeleton. For example, the antorbital sinus has a ventromedial diverticulum that pneumatizes the maxillary palatal process; although a similar maxillary sac was reported above in alligators, the two are not homologous.

The most voluminous diverticulum of the antorbital sinus is the suborbital sinus, which in ostriches is connected more directly to the maxillary sac than to the main antorbital sinus (Fig. 4). This relationship pertains also to the juvenile ostrich (OUVC 10504) in the latex-injected sample, but all of the other birds in the sample in which the sinuses were injected with latex show the situation where the suborbital sinus emerges directly from the antorbital sinus. The suborbital sinus in all the birds studied here has a number of subsidiary diverticula, the most consistent ones being a lacrimal sac (pneumatizing the lacrimal bone in *Struthio*; Fig. 4), a preocular sac in front of the eyeball, and an intermuscular sac that interleaves between different bellies of the jaw adductor musculature (e.g., components of the pterygoideus, protractor, and adductor mandibulae externus muscles; Holliday and Witmer, 2007). Moreover, in *Struthio* (and most other ratites) there is a prominent sac that lies atop the pterygoid bone (which is thus pneumatized by it) and then passes dorsally over the basipterygoid processes to project into the middle ear region, although it does not communicate with the tympanic cavity (Fig. 4).

Struthio and probably other birds have another paranasal air sinus in addition to the antorbital sinus. The fronto-ethmoidal sinus, reported here for the first time, derives as a diverticulum from the nasal cavity proper near its caudodorsal apex, within the olfactory region of the nasal cavity (Fig. 4). The sinus ostium is topographically similar in position to the spheno-ethmoidal recess of human anatomy, but the two are certainly not homologous. From this region, both the frontal bone and the mesethmoid bone (an ossification of the cartilaginous septum) are pneumatized by the fronto-ethmoidal sinus. Witmer (1990, 1995b) previously suggested that these bones were pneumatized by a diverticulum of the antorbital sinus, but CT scanning now shows that this is not the case for *Struthio* and perhaps not for other birds either.

Extinct Nonavian Theropods: *Majungasaurus* and *Tyrannosaurus*

Given that birds are theropod dinosaurs, it should not be surprising that the paranasal sinuses of extinct theropods, such as *Majungasaurus* and *Tyrannosaurus*, resemble those of the ostrich more than those of the alligator. The paranasal air sinuses of theropods in general were surveyed previously (Witmer, 1997a,b), and the reader is referred to those analyses for an account of the diversity of theropod pneumatic accessory cavities. Likewise, Sampson and Witmer (2007) provided detailed descriptions of the individual pneumatic spaces of *Majungasaurus*, which will not be repeated here. Instead, those previous studies will be used as a springboard, and integrate these findings with new analyses based on new visualizations of all the pneumatic structures together and in place. In general, the antorbital paranasal systems of probably all theropods resemble that outlined above for the ostrich. That is, there is a well developed (in some cases, enormous) antorbital cavity bounded by the maxilla, lacrimal, and palatine, and also often the jugal (zygomatic of mammalian anatomy) and/or nasal bones. As in extant theropods (i.e., birds), the bony antorbital cavity is open laterally such that, in life, the external antorbital fenestra was covered only by skin. Although once controversial, there is now

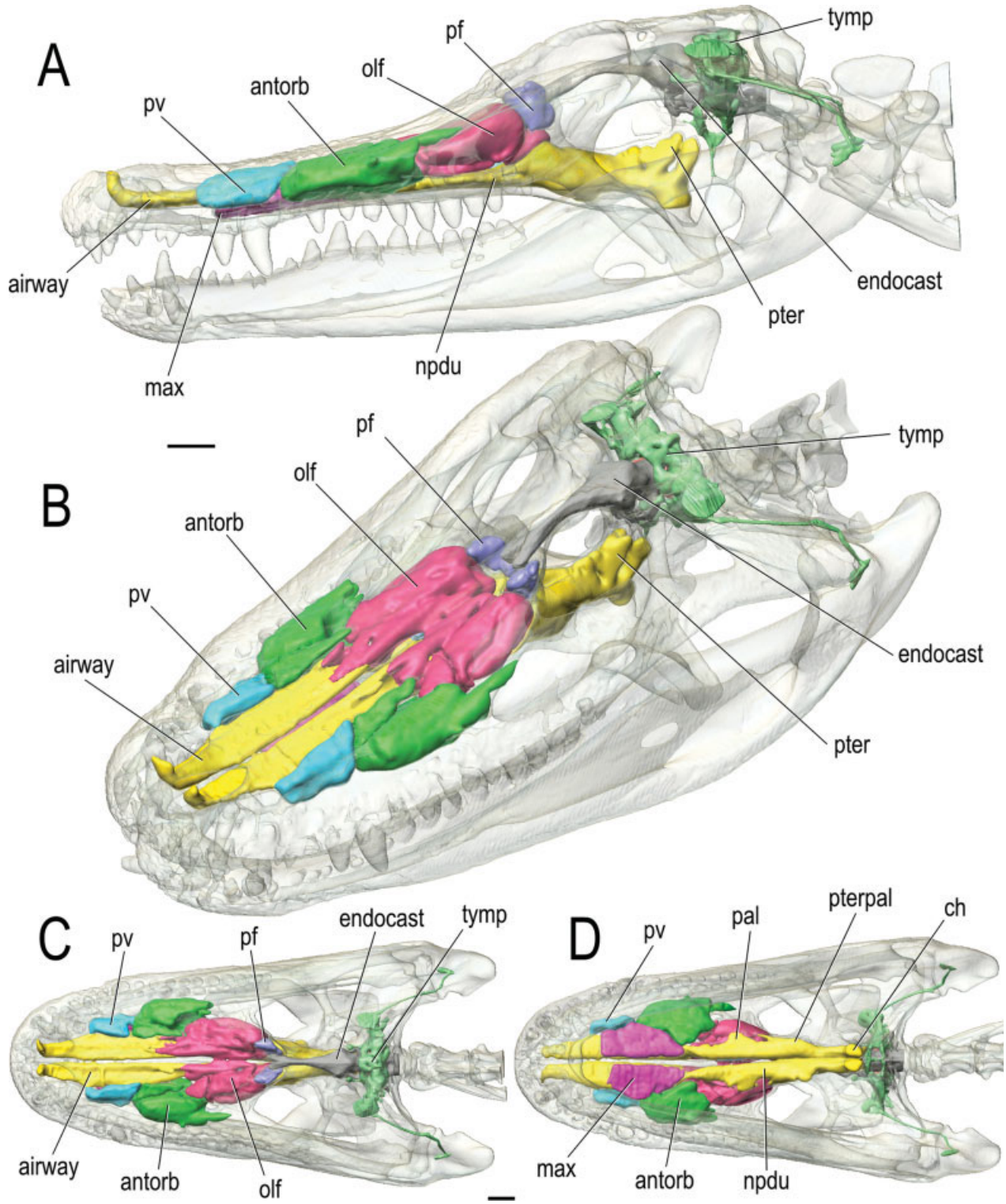

Fig. 3. Paranasal sinuses and other cephalic components of an American alligator (*Alligator mississippiensis*, OUVC 9761) based on CT scanning followed by segmentation and 3D visualization. Bone is rendered semitransparent. **A:** Left lateral view. **B:** Left rostrodorsolateral view. **C:** Dorsal view. **D:** Ventral view. Scale bars = 2 cm.

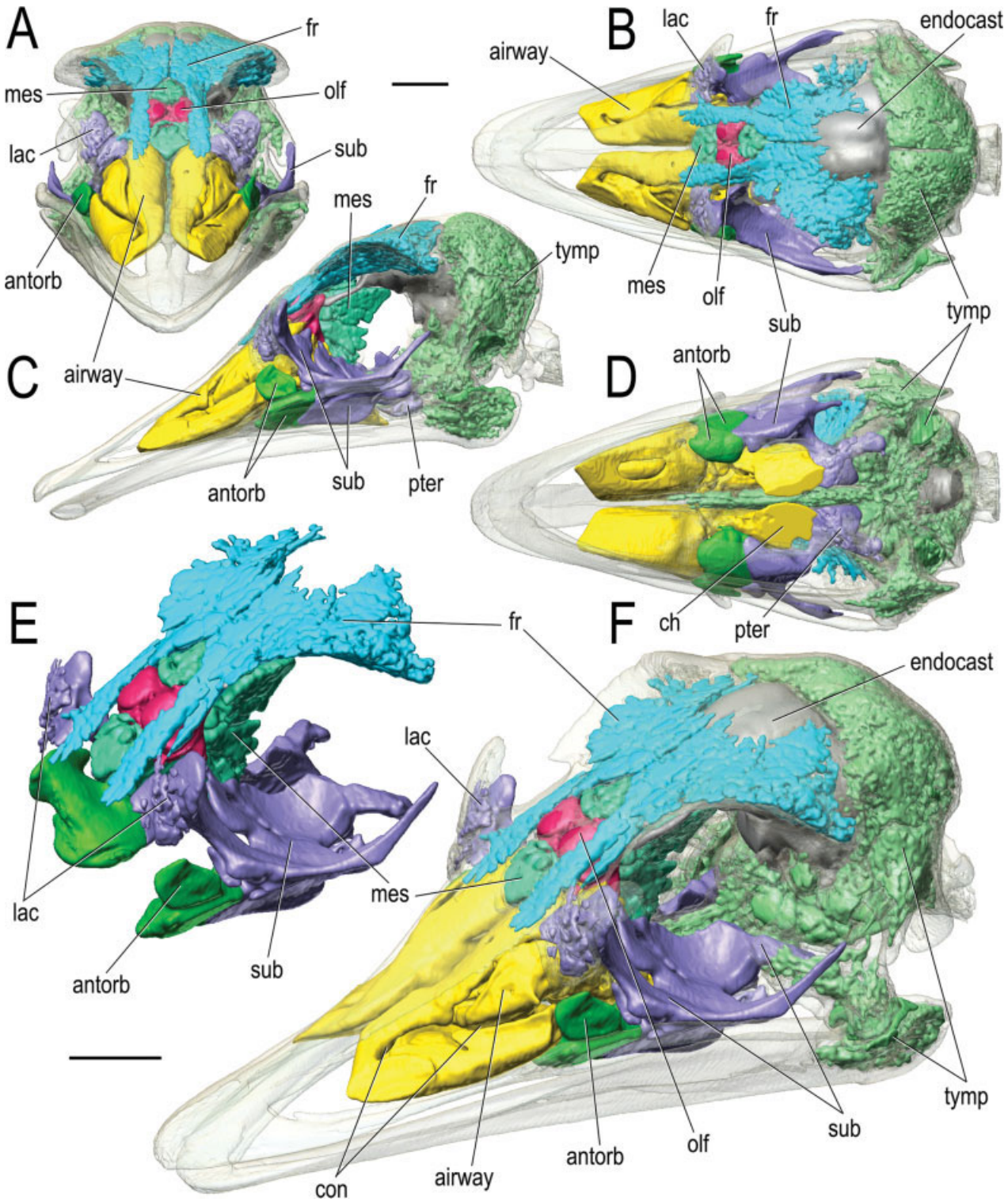

Fig. 4. Paranasal sinuses and other cephalic components of an ostrich (*Struthio camelus*, OUVC 10491) based on CT scanning followed by segmentation and 3D visualization. Bone is rendered semitransparent. **A:** Rostral view. **B:** Dorsal view. **C:** Left lateral view. **D:** Ventral view. **E:** Isolated paranasal sinuses in left rostrodorsolateral view. **F:** Left rostrodorsolateral view. Scale bars = 2 cm.

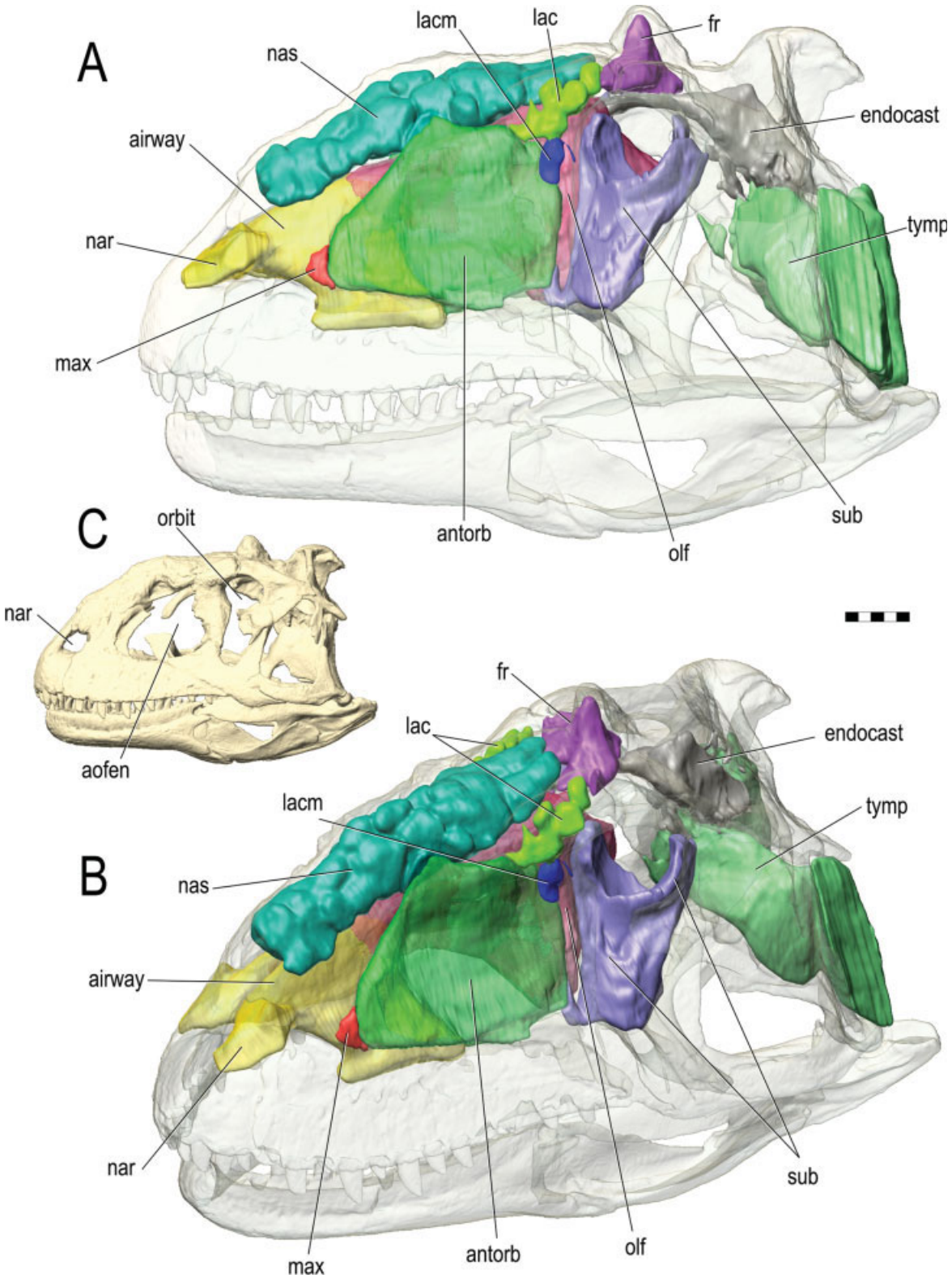

Fig. 5. Paranasal sinuses and other cephalic components of *Majungasaurus crenatissimus* (FMNH PR2100) based on CT scanning followed by segmentation and 3D visualization. Bone is rendered semitransparent (except in **C**), as is the nasal cavity (airway and olfactory region). **A:** Left lateral view. **B:** Left rostrodorsolateral view. **C:** Skull in left lateral view. **D:** Ventral view. **E:** Rostral view. **F:** Dorsal view. Scale bars = 5 cm.

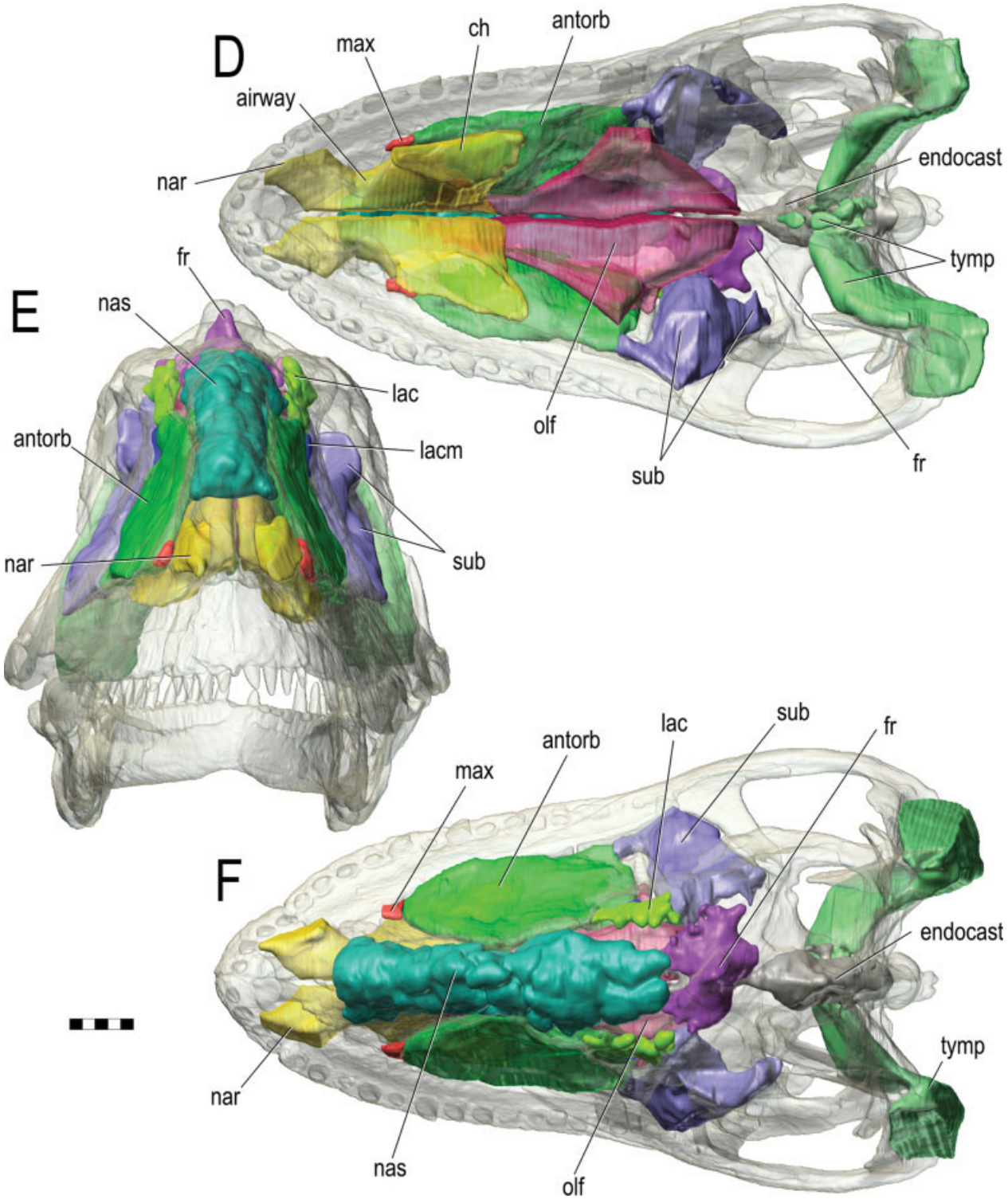

Figure 5. (continued)

abundant evidence that the antorbital cavity of extinct archosaurs was causally linked to the presence of the antorbital paranasal air sinus, just as in extant archosaurs, and some of the strongest evidence comes from theropods where there are numerous examples of accessory cavities that open directly into the antorbital cavity (Witmer, 1997a). These accessory cavities have the same smooth-walled, strutted appearance of pneumatic cav-

ities as seen in extant archosaurs and mammals, and the well-preserved fossils of *Majungasaurus* serve well as an exemplar.

In *Majungasaurus* (Fig. 5), the antorbital sinus occupied the main antorbital cavity, bounded by the maxilla, jugal, lacrimal, nasal, and palatine bones. *Majungasaurus* and other abelisaurids are unusual among theropods in that the facial bones are highly sculptured due to mineralization of the overlying periosteum and dermis (Sampson and Witmer, 2007). This mineralization of the integument had the effect of somewhat diminishing the size of the external antorbital fenestra because of overgrowth at the bony margins. This overgrowth also eliminated the smooth fossa on the lateral surfaces of many of the surrounding bones caused by the sinus epithelium and retained in most other theropods. In *Majungasaurus*, the pneumatic fossa is retained on only the rostral portion of the maxilla and small parts of the nasal and lacrimal. As reconstructed here for the first time, the epithelial antorbital sinus was a more or less lenticular structure, presumably flattened laterally where it would have been covered by skin and peaked medially as it conformed to the airway (the peak represents the vomeropterygoid or choanal process of the palatine bone).

The antorbital sinus of *Majungasaurus* had five demonstrable subsidiary diverticula (Fig. 5). (1) A very small maxillary sac extended from the rostral vertex of the antorbital sinus into the ascending ramus of the maxilla. Most theropods had much larger pneumatic sinuses in the maxilla, and the generally small space in abelisaurids is probably a primitive attribute. (2) What represents a dramatic derived character for *Majungasaurus*, even among abelisaurids, is the extensive paranasal sinus in the nasal bones. The nasals are fused in *Majungasaurus*, and the element is markedly inflated by the sinus, which entered the bone laterally at its mid-length via a large pneumatic foramen. The nasal sinus was incompletely partitioned by struts and septa, resulting in its lobular form. (3) At its caudodorsal vertex, the antorbital sinus sent a diverticulum into the lacrimal bone. In most theropods, the lacrimal pneumatic aperture is visible laterally, but overgrowth of bone by mineralization of the integument obscured the aperture in *Majungasaurus*, diverting it to open rostrally. The lacrimal sinus proper expanded within the body of the bone, and, again, incomplete bony partitions produced 3–4 rounded pneumatic chambers. (4) The lacrimal bone received another, separate diverticulum from the antorbital sinus. This medial lacrimal sinus is relatively small in *Majungasaurus*, as it is in most theropods. (5) The final diverticulum of the antorbital sinus to be considered here is the suborbital sinus, extending caudally into the orbit. The evidence for the suborbital sinus is the weakest simply because the diverticulum is not fully enclosed within bone, and the details of its shape indicated in Fig. 5 are partly conjectural (modeled on the avian sac) and partly based on the space available after jaw adductor musculature is reconstructed (Holliday, 2006). However, there is evidence for a preocular sac of the suborbital sinus in *Majungasaurus* in that there is a canal connecting the lacrimal sinus proper with the orbit (well dorsal to and separate from the nasolacrimal canal). Such a canal has been identified in other theropods (e.g., *Allosaurus fragilis*; Witmer, 1997a; Sampson and Witmer, 2007). Moreover, other theropods (e.g., dromaeosaurids; see Witmer, 1997a) show further evidence for a suborbital diverticulum, such as pneumatic apertures on the dorsal surfaces of certain palatal bones, much as noted above for the sinuses within the pterygoids of ostriches.

There is no positive evidence in *Majungasaurus* or currently any other theropod for the other paranasal sinus reported above for birds, the fronto-ethmoidal sinus. Nevertheless, *Majungasaurus* indeed appears to have had air sinuses within the frontal bones, although they are problematic for a variety of reasons (Sampson and Witmer, 2007). Not only are they variable among specimens (they happen to be largest in FMNH PR2100; Fig. 5), but the source of the pneumatic diverticulum is not entirely clear. There are no pneumatic apertures in the frontals that would be consistent with a fronto-ethmoidal sinus, and in fact the best candidates for pneumatic ostia are apertures associated with the articular surface where the frontal sutures to the lacrimal. This scenario would require that the paranasal sinus in the lacrimal would have crossed the suture to pneumatize the frontal. Cases of cross-sutural pneumatization abound in mammals, crocodilians, and birds (the "extramural" pneumatization of Witmer, 1990). There is some evidence for this hypothesis in *Majungasaurus* (Sampson and Witmer, 2007), but requires further testing with additional fossil material. Significantly, frontal sinuses were identified in another theropod (*Ceratosaurus*, a close relative of abelisaurids; Witmer et al., 2004; Sanders and Smith, 2005; Sampson and Witmer, 2007), and, armed with a CT scanner and the proper search image, more cases may be discovered, although frontal sinuses can be shown definitively to be absent in a number of theropods that the authors have sampled.

In *Tyrannosaurus* (Fig. 6), the antorbital sinus and its subsidiary diverticula are generally organized in a similar fashion to those of *Majungasaurus* and other theropods. For example, the antorbital sinus again was a relatively extensive but mediolaterally thin sac that extended to the margins of the external antorbital fenestra, bounded largely by the maxilla, lacrimal, and jugal bones. Unlike *Majungasaurus*, the nasal bone does not participate in the antorbital cavity in tyrannosaurids, and so is not pneumatic. This variability in the presence of paranasal sinuses within the nasal bone characterizes theropods as a whole, and even close relatives may have different states (e.g., among velociraptorine dromaeosaurid maniraptorans, *Deinonychus antirrhopus* has a nasal sinus whereas *Velociraptor mongoliensis* lacks it).

The antorbital sinus of *Tyrannosaurus* is roughly triangular in lateral view, and a diverticulum extends into bone at each vertex. The promaxillary sinus, located at the rostral vertex, will be discussed along with the other maxillary sinuses in the next paragraph. The jugal sinus was located at the caudoventral vertex, and excavated a large aperture in the jugal bone before pneumatizing the body and rami of the bone. The lacrimal diverticulum proper evaginated at the caudodorsal vertex of the antorbital sinus, just as it did in *Majungasaurus*. Indeed, the lacrimal sinus proper was among the most consistent paranasal sinuses in theropods, and *Tyrannosaurus* exhibits an extensive series of interconnected chambers within the body of the lacrimal, as well as a large medial lacrimal sinus.

The presence of antorbital sinus diverticula into the maxilla is also almost universal in theropods, but

whereas *Majungasaurus* had only a very small sinus, *Tyrannosaurus* had extensive maxillary sinuses (Fig. 6). Moreover, *Tyrannosaurus* displays the derived condition of having had two separate diverticula into the maxilla (Witmer, 1997a,b). As mentioned, the promaxillary sinus evaginated from the rostral vertex of the antorbital sinus, passing through an aperture in the maxilla to excavate a series of bony chambers known collectively as the promaxillary recess. In *Tyrannosaurus*, the promaxillary recess is huge, strutted, and septate, and pneumatizes much of the ascending ramus. Just caudal to the promaxillary sinus, another antorbital sinus diverticulum evaginated medially into the maxilla. This diverticulum produced a large aperture (the maxillary fenestra) and excavated a bony cavity known as the maxillary antrum. Although the promaxillary recess and maxillary antrum of most disarticulated tyrannosaurid maxillae appear to be open medially, intact specimens (e.g., FMNH PR2081; Brochu, 2003) reveal that these sinuses were covered with a thin lamina of bone medially, such that the contralateral bony chambers virtually touched each other (separated only by the cartilaginous septum) and diverted the nasal airway dorsally over the sinus chambers. The promaxillary and maxillary antral sinuses also had a series of diverticula directed ventrally into the body of the maxilla between the teeth (the interalveolar recesses; Witmer, 1997a). The maxillary antral sinus had yet another diverticulum, passing caudally through an aperture in the back wall of the antrum (the postantral fenestra) to reach the palatine bone, which it invaded through one or more apertures. The resulting palatine sinuses of most *Tyrannosaurus* specimens inflated the bone to the point that it often seems puffy and misshapen. Thus, air reached the palatine bone of tyrannosaurids via a circuitous route: from the nasal cavity to the antorbital sinus to the maxillary antral sinus and finally to the palatine sinus.

The final diverticulum of the antorbital sinus is the suborbital sinus (Fig. 6), the precise form of which, as in *Majungasaurus*, is somewhat speculative, because it largely passed between soft tissues. Again as in *Majungasaurus*, there is good evidence for a preocular sac of the suborbital sinus in *Tyrannosaurus* in that there is a canal connecting the orbit with a pneumatic sinus in the lacrimal (the medial lacrimal sinus, in this case); Molnar (1991) had interpreted this canal as the nasolacrimal canal, but the latter takes a different course (through the lacrimal's rostral ramus) in all theropods, including tyrannosaurids. Witmer (1997a,b) noted the presence of two problematic pneumatic cavities in theropods, both of which *Tyrannosaurus* had. The first is in the squamosal bone (also found in ornithomimosaurs; Fig. 6). The cavity is clearly pneumatic in that it is partially partitioned by struts and septa. The problem is whether the pneumatic diverticulum derives from the suborbital diverticulum of the antorbital sinus or from the nearby paratympanic sinuses. As Witmer (1997a,b) discussed, there is insufficient evidence to make a clear choice, but a caudodorsal intermuscular diverticulum of the suborbital sinus is perhaps more likely. The second cavity is in the ectopterygoid bone (Fig. 6). Again, this cavity is clearly pneumatic (see also Witmer and Ridgely, in press), but the source of the pneumatizing diverticulum is even more uncertain.

In summary, the paranasal air sinuses of nonavian theropod dinosaurs, as typified by *Majungasaurus* and *Tyrannosaurus*, are very extensive, pneumatizing many or most of the facial and palatal bones, and, in some cases (e.g., the nasal of *Majungasaurus*, the palatine of *Tyrannosaurus*), positively inflating the bones. Moreover, the systems are remarkably complex. Despite there being just a single demonstrable paranasal sinus arising from the nasal cavity proper (the antorbital sinus), there are numerous subsidiary diverticula of that one sinus, which may themselves have subsidiary diverticula. In *Tyrannosaurus*, the end result is as many as 10 named paranasal sinuses.

Armored Dinosaurs: *Panoplosaurus* and *Euoplocephalus*

The snouts of both nodosaurid (e.g., *Panoplosaurus*) and ankylosaurid (e.g., *Euoplocephalus*) ankylosaurians are highly transformed compared with the theropods discussed earlier. The challenge of ankylosaurs is that, being armored dinosaurs, their skulls are covered with thickened roofing bones and ornamented dermal ossifications (osteoderms) that are fused to the skull and close the external antorbital fenestra. As a result, their skulls have often seemed as impregnable to scientific study as they were to predatory attack, requiring broken, incomplete, or sawn specimens to provide information on internal structure. Nevertheless, paleontologists have always regarded ankylosaurs as having had sometimes extensive paranasal air sinuses. For example, in the initial announcement naming the group, Brown (1908, p 188–190) observed "many large continuous chambers in the upper part of the skull [of *Ankylosaurus*]. . . that are bilaterally symmetrical and may have been air chambers, comparable to the sinuses in Proboscidean [i.e., elephant] skulls." Since that time, numerous researchers have identified sometimes complex sinuses in various ankylosaurs (e.g., Maryańska, 1977; Coombs, 1978; Tumanova, 1987; Coombs and Maryańska, 1990; Witmer, 1997a,b). CT scanning has opened up new opportunities (Hill et al., 2003; Vickaryous and Russell, 2003; Vickaryous et al., 2004; Kilbourne and Carpenter, 2005; Vickaryous, 2006), but the present study is the first to go beyond looking at CT slices to use digital segmentation tools and 3D visualization. These approaches shed new light on the course of the nasal airway and the disposition of the paranasal sinuses.

Nodosaurids such as *Panoplosaurus* (Fig. 7) are generally regarded as more generalized or "primitive" than ankylosaurids (Coombs and Maryańska, 1990; Hill et al., 2003; Vickaryous et al., 2004), in part because nodosaurids were thought to lack the complicated nasal cavities and paranasal sinuses of ankylosaurids (Coombs, 1978; Coombs and Maryańska, 1990). More recent studies seemed to confirm that indeed the airway was a simple straight tube running from nostril to choana, although maybe there was a small paranasal air sinus laterally within the maxilla (Witmer, 1997a; Vickaryous et al., 2004; Vickaryous, 2006; see comments below on the authors' preliminary findings on *Edmontonia*). However, the CT-based studies of *Panoplosaurus* (ROM 1215) presented here suggest that the nasal airway of this nodosaurid was much more complicated than previously thought. Completely enclosed in bone, the airway of

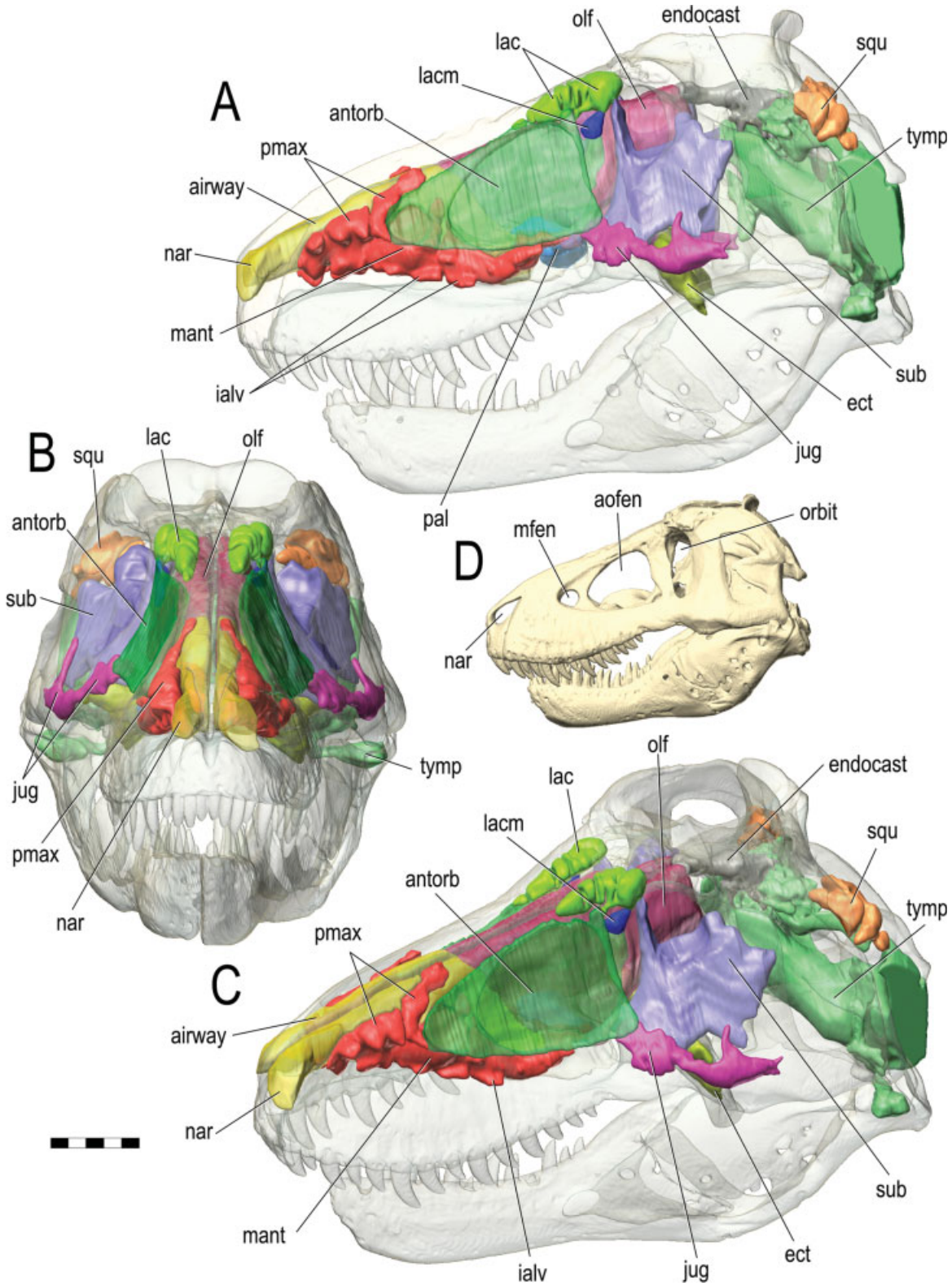

Fig. 6. Paranasal sinuses and other cephalic components of *Tyrannosaurus rex* (skull based on FMNH PR2081; soft-tissue components from several specimens, see text) based on CT scanning followed by segmentation and 3D visualization. Bone is rendered semitransparent (except in **D**), as is the nasal cavity (airway and olfactory region). **A:** Left lateral view. **B:** Rostral view. **C:** Left rostrodorsolateral view. **D: Skull in left lateral view. E:** Dorsal view. **F:** Ventral view. **G:** Right side of sagittally sectioned head in medial view. Scale bars = 20 cm.

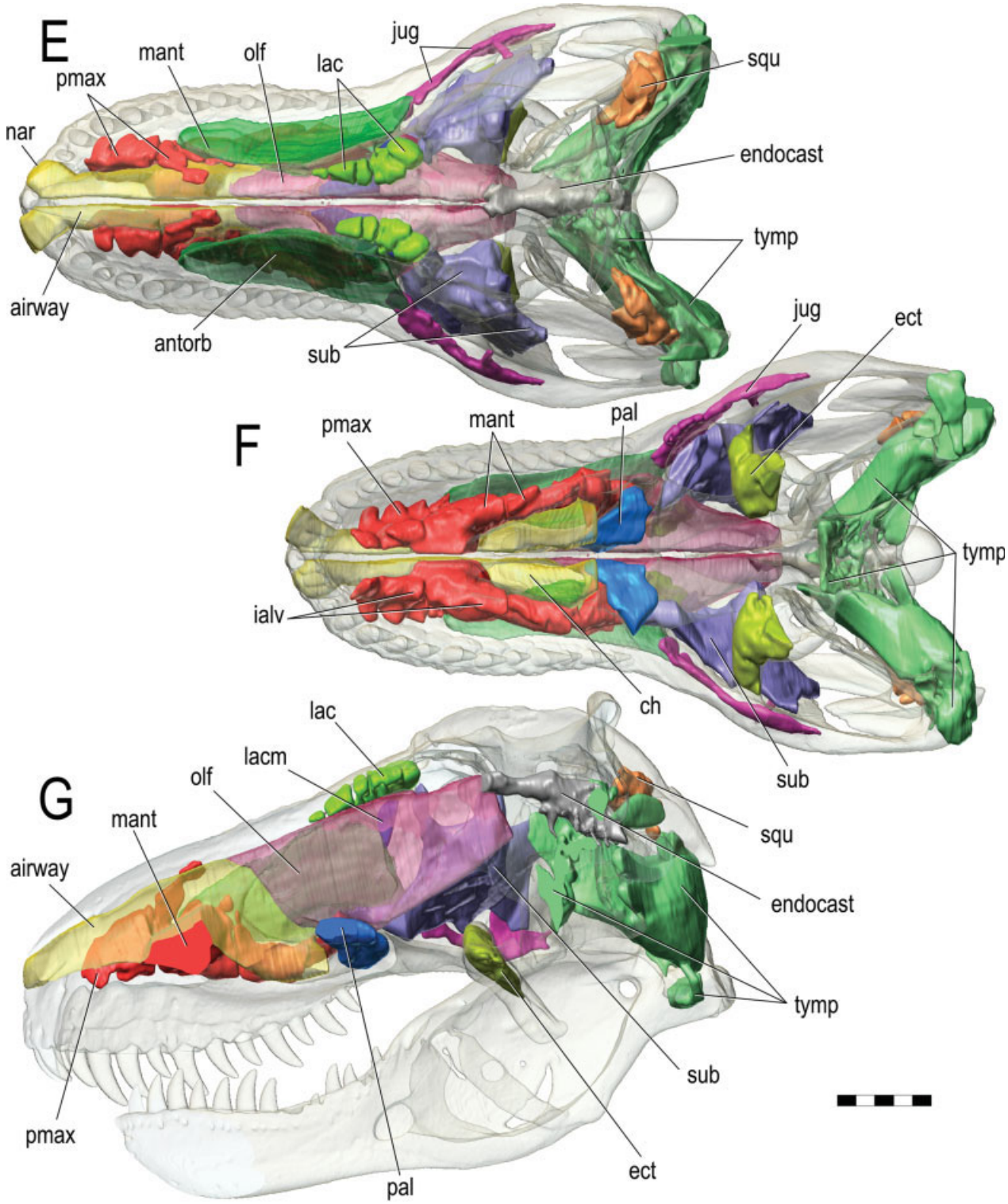

Figure 6. (continued)

ROM 1215 takes a series of twists and turns that ultimately comprise two separate 360° loops, each in a different plane. The course of the airway will be described in relation to the "alert" or habitual posture of the head, which is strongly down-turned (Fig. 7), as reconstructed from the orientation of the lateral semicircular canal of the endosseous labyrinth (for justification, see Witmer et al., 2003, 2008; Sereno et al., 2007). Starting rostrally

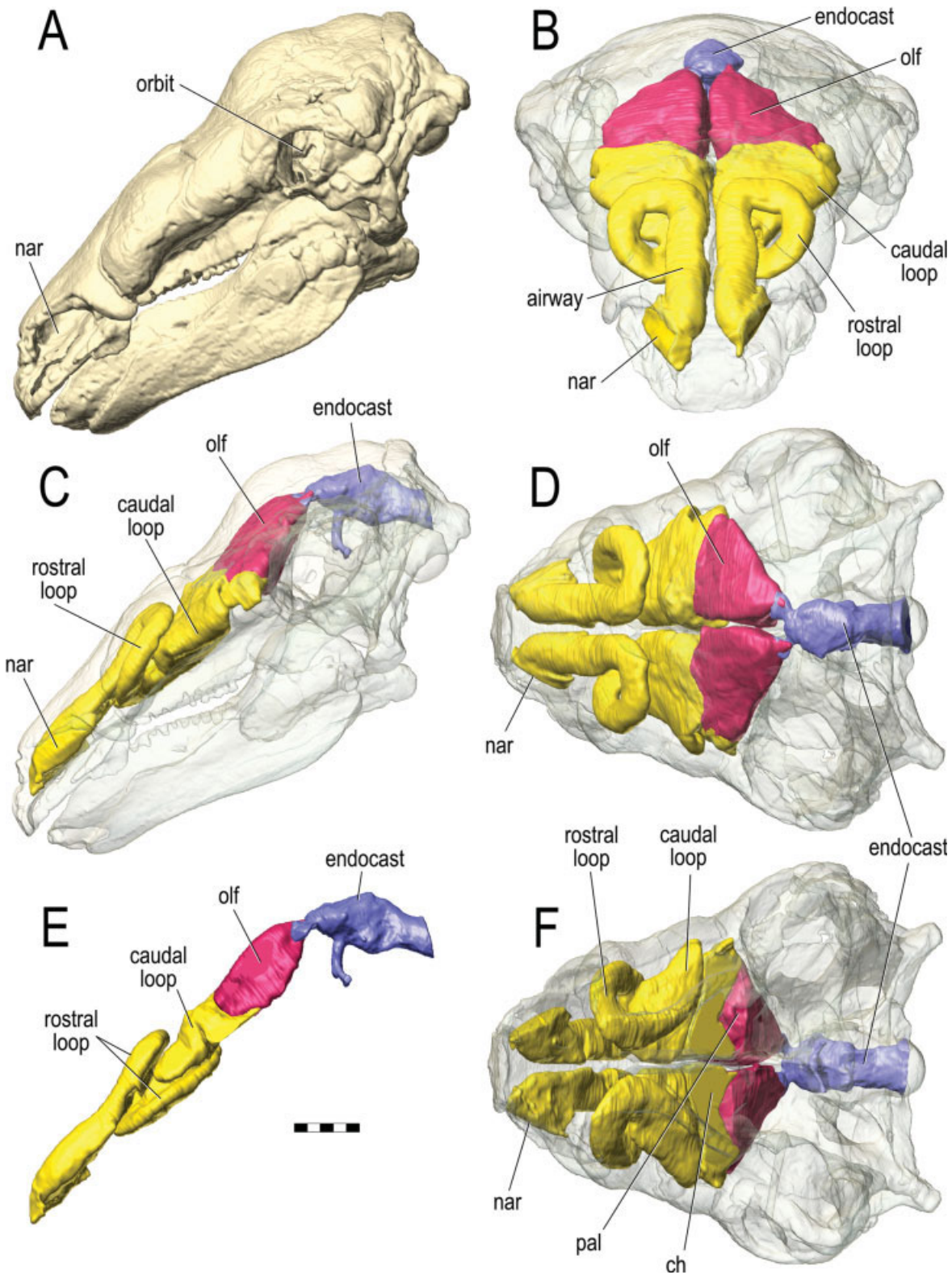

Fig. 7. Paranasal sinuses and other cephalic components of *Panoplosaurus mirus* (ROM 1215) based on CT scanning followed by segmentation and 3D visualization. Bone is rendered semitransparent (except in **A**). **A:** Skull in left lateral view. **B:** Rostral view. **C:** Left lateral view. **D:** Dorsal view. **E:** Right side of sagittally sectioned head in medial view with soft-tissue components isolated. **F:** Ventral view. **G:** Left rostrodorsolateral view. **H:** Isolated and semitransparent nasal cavity in left rostrodorsolateral view, revealing the course of the nasal airway (arrow). **I:** Same in left lateral view. Scale bars = 5 cm.

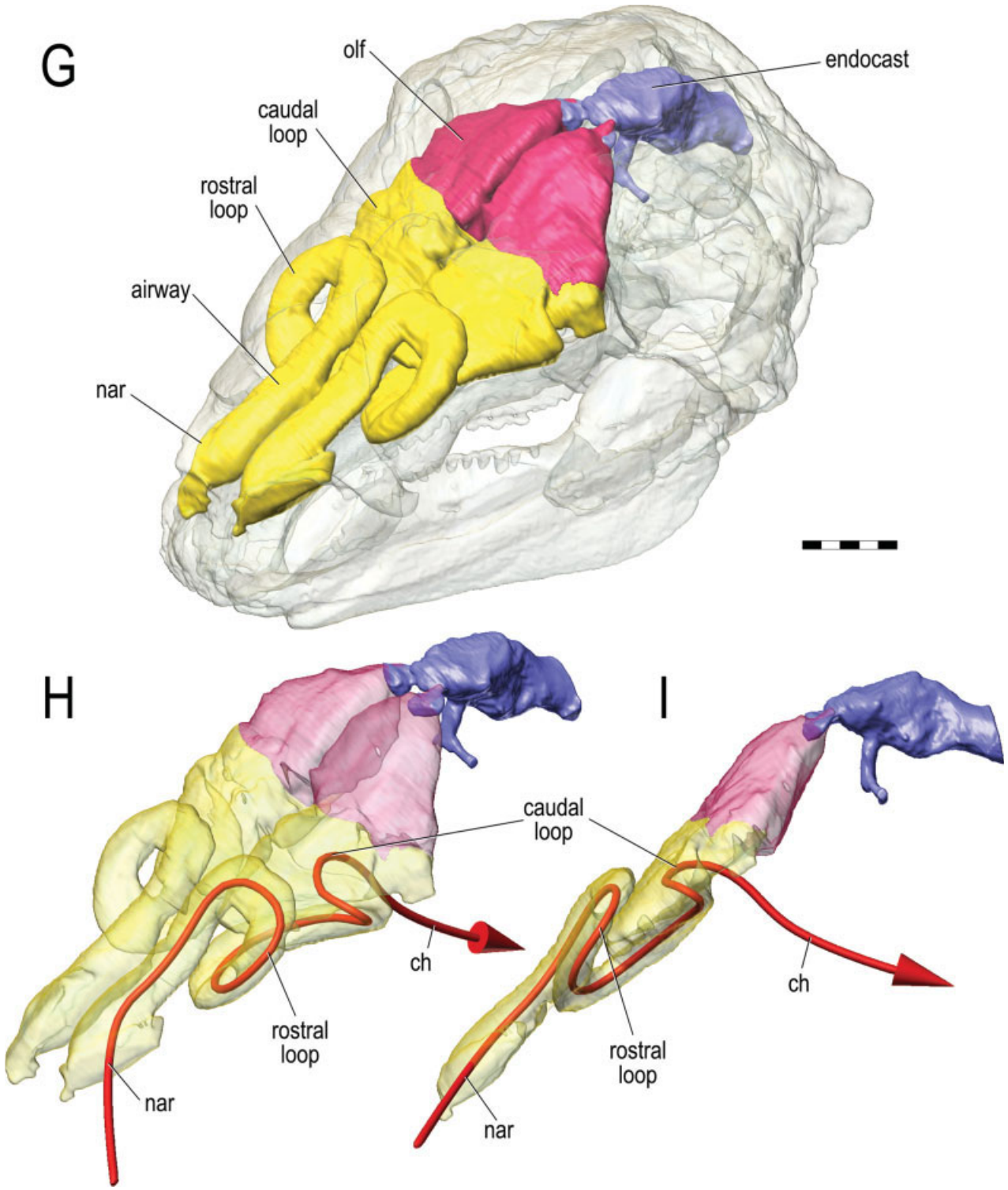

Figure 7. (continued)

at the nostril, the airway ascends directly caudodorsally adjacent to the median septum. It then begins the rostral loop, turning laterally and then rostroventromedially, completing the loop directly below the ascending tract. The airway then ascends again, passing caudodorsolaterally, after which it makes the second loop, arcing caudoventromedially to the choana. This unexpected pattern of complex looping is remarkably symmetrical,

and the osteological evidence is very clear, in that there are a series of bony lamina segregating the various loops.

The next question becomes, what is the status of any paranasal sinuses in the ROM 1215 skull of *Panoplosaurus*? Virtually all of the nasal cavity space rostral to the choana can be attributed to the main nasal airway. Perhaps the part of the nasal cavity medial to the caudal loop and rostral to the choana could be regarded as a sinus based on the fact that it is somewhat out of the course of the main airway. Indeed, there could have been cartilaginous subdivision of that chamber (unpreserved in the fossil), although there is no real evidence for it, and the chamber is fully confluent with the main nasal cavity. The best case for paranasal sinuses in *Panoplosaurus* (at least ROM 1215) comes from the region behind the choana. This space is here regarded as the olfactory region of the nasal cavity (as opposed to the respiratory region rostral to it) based on the presence within this chamber of a complex and symmetrical series of delicate, often scroll-like laminae, resembling the olfactory turbinates of many amniotes. Maryańska (1977) and Tumanova (1987) previously identified similar "ethmoturbinals" in some Asian ankylosaurids. Moreover, this chamber in ROM 1215 directly contacts the region where the olfactory lobes of the brain would have been located (Fig. 7). The relevance for paranasal sinuses is that this olfactory chamber communicates with chambers within the palatine bone, which itself has a large aperture opening into the choanal region. This palatine aperture has previously been regarded as leading to sinus chambers in ankylosaurids (Maryańska, 1977; Tumanova, 1987; Hill et al., 2003; Vickaryous and Russell, 2003; Vickaryous et al., 2004), but *Panoplosaurus* (ROM 1215) represents its first record for nodosaurids.

These findings for *Panoplosaurus* (ROM 1215) stand in stark contrast to those of Witmer (1997a) and Vickaryous (2006; see also Vickaryous et al., 2004), who identified a simple straight airway and a small paranasal sinus in the presumably very closely related nodosaurid *Edmontonia*. Witmer's (1997a) interpretation can be largely discounted, because it was based on a single transverse section through a broken specimen (AMNH FR 3076), and in fact, the arrangement of the nasal cavity in the section agrees very well with the caudal loop of the airway observed here for ROM 1215, suggesting that AMNH FR 3076 may have had a similarly looped airway. Vickaryous' (2006) interpretations of a straight airway and paranasal sinus were based on CT slices through a well-preserved *Edmontonia* skull (AMNH FR 5381), the same skull that was scanned late in the present study and for which preliminary findings are available. These findings largely affirm Vickaryous' observations, and the differences cannot be attributed to ontogeny (ROM 1215 and AMNH FR 5381 are similarly sized), pathology, or preservation. Rather, we suggest that these are real (and potentially profound) differences between ROM 1215 and AMNH FR 5381. However, although Vickaryous (2006, p 1011) stated that AMNH FR 5381 shows "no further signs of subdivision, internal bracing, or conchae within either the nasal cavities or paranasal sinus cavities," the new findings reveal thin bony (or mineralized) laminae within the main nasal cavity, as well as suggestive heterogeneities in the enclosed rock matrix, that may indicate that some complexity of the airway may have been present but not fully mineralized. Also, the new scan data show that AMNH FR 5381 indeed has olfactory conchae similar to those reported here for *Panoplosaurus*. Significantly, Vickaryous (2006) suggested that the paranasal sinus of *Edmontonia* connected not with the nasal cavity proper but rather with the nasal vestibule via an aperture separate from but adjacent to the nostril. He identified (and we can confirm) this "paranasal aperture" in *Edmontonia* skulls other than AMNH FR 5381. However, AMNH FR 5381 itself lacks the aperture and, according to the new scan data, the paranasal sinus joins the main nasal cavity well behind the vestibule. The ROM 1215 skull of *Panoplosaurus* also clearly lacks such a paranasal aperture. Unfortunately, to the knowledge of the authors, skulls with a demonstrable paranasal aperture have not been CT scanned.

Similar apertures within the nasal vestibule are well known in some ankylosaurids (Maryańska, 1977), but, as Hill et al. (2003) documented in their CT-based study of *Pinacosaurus*, these narial apertures do not open into a "paranasal sinus" adjacent to the nasal cavity proper (i.e., the condition Vickaryous postulated for the nodosaurid *Edmontonia*). Rather, these narial apertures open into a large air sinus restricted to and inflating the premaxillary bone and, in particular, its palatal process. Thus, these premaxillary sinuses indeed constitute paranasal air sinuses but are of a variety that is very rare in amniotes, namely, a diverticulum from the nasal vestibule rather than from the more common source of the nasal cavity proper.

The ankylosaurid *Euoplocephalus* (Fig. 8) presents a situation very similar to that for *Panoplosaurus* in that full segmentation and 3D visualization of the CT data produced results that require a revision of previous notions of nasal anatomy. As noted above, many researchers have interpreted ankylosaurids as having had numerous paranasal air sinuses, as well as a more complex airway that made a sagittal S-loop through the snout. Most of these observations were made based on broken specimens, as well as a transversely sawn specimen of *Euoplocephalus* (AMNH FR 5403) that formed the basis of Coombs (1978) very influential work. Witmer (1997a) studied the same specimen and affirmed Coombs' observations and interpretations. Vickaryous and Russell (2003; see also Vickaryous et al., 2004) presented important new CT data (publishing five slices) of a different specimen of *Euoplocephalus*, again supporting the S-loop airway and paranasal air sinuses. The new CT data for AMNH FR 5405 presented here, as well the CT data for the sawn specimen (AMNH FR 5403) generated late in the present study, generally agree with other specimens and Vickaryous' published slices, suggesting that these specimens of *Euoplocephalus* are all anatomically consistent.

The results for AMNH FR 5405 presented here, however, support neither the S-loop airway nor the maxillary sinus of Coombs (1978), Witmer (1997a), or Vickaryous and Russell (2003). The new findings suggest that the airway of *Euoplocephalus* took an almost absurdly complex looping pathway (Fig. 8), by comparison making the double 360° loops of *Panoplosaurus* look relatively simple. However, there are perhaps some fundamental similarities in that *Euoplocephalus* also can be interpreted as having rostral and caudal loops of the airway.

Again, the course of the airway will be described with the skull oriented in the alert posture (i.e., with the lateral semicircular canal horizontal), which produces a somewhat more down-turned posture than typically portrayed. Previous workers had suggested that the S-loop airway took a dorsomedial course, hugging the median septum and skull roof before turning rostrally and ventrally to curve around palatal shelves on its way to the choana. According to the new findings, that dorsomedial course is initially true, but the airway then encounters a lamina of bone that diverts it ventrolaterally. It then makes a quick rostral turn, passing dorsomedially after which it then passes rostrally again before taking a long caudoventrolateral course though the maxilla before making another rostrodorsal loop. [It is worth noting here that this maxillary course of the airway represents the "maxillary sinus" of previous authors. In fact, Witmer's (1997a, p 31) photograph of AMNH FR 5403 and Vickaryous and Russell's (2003) CT slices both display the "maxillary sinus" as being horizontally pinched if not fully subdivided, no doubt reflecting the rostrodorsal loop at the caudal end of the maxillary course of the airway.] The looping just described in some ways is comparable to the rostral loop of the airway described above for *Panoplosaurus*, albeit much more complex. Picking up the course of the airway, it enters a caudal loop that is more directly comparable to that of *Panoplosaurus*. The airway comes out of the rostrodorsal loop within the maxilla and passes caudodorsomedially. As it approaches the midline, the airway turns directly caudally adjacent to the median septum and below the skull roof (the caudal dorsomedial portion of the airway in the old S-loop model), passing through part of the olfactory region (again as defined by the presence of a chamber containing scroll-like turbinates adjacent to the olfactory lobes of the brain) before turning rostroventrally on its way to the choana. Preliminary segmentation of the airway of AMNH FR 5403 shows that it is virtually identical to that just described for AMNH FR 5405.

Thus, there are potentially no typical paranasal sinuses within the snout of *Euoplocephalus* (apart from the sinuses within the palatine that lead to the olfactory chamber, as in *Panoplosaurus* and many other ankylosaurians; see above). Instead of sinuses, the snout houses a highly convoluted airway. However, an apparent incongruity arises with the identification in *Euoplocephalus* of a premaxillary "paranasal aperture" for the "maxillary sinus" (Coombs and Maryańska, 1990; Vickaryous and Russell, 2003; Vickaryous et al., 2004). This aperture would be similar to the "paranasal aperture" identified for some specimens of *Edmontonia* by Vickaryous (2006) or the narial apertures that lead into the premaxillary sinuses in *Pinacosaurus* (Hill et al., 2003). There are, however, no premaxillary sinuses in *Euoplocephalus*. According to the findings presented here, the putative aperture opens into the airway and indeed into that portion that passes through the maxilla. However, on closer inspection of AMNH FR 5405, the "aperture" is not truly separated from the bony nostril on either side but rather is confluent with it. Thus, it is possible that the supposed paranasal aperture is just a part of the true nasal opening. Indeed, it is not entirely clear that other *Euoplocephalus* have a second aperture within the narial region. Nevertheless, the incongruity remains, pending resolution with other fossil specimens.

Finally, a medial channel in the snout was discovered that passes caudodorsally from the rostralmost part of the airway directly to the caudal dorsomedial part of the airway, and it might seem that this channel could "short-circuit" our convoluted airway. However, when followed rostrally, this median channel leads to a series of neurovascular canals in the premaxilla, suggesting instead that this channel conducts the medial nasal branches of the ophthalmic nerve and ethmoidal vessels. Indeed, these structures take a similar course in extant birds and crocodilians (Witmer, 1995b). The medial nasal neurovascular channel is quite large in diameter, suggesting that the vascular component was extensive. Preliminary analysis of AMNH 5403 confirms that this medial channel is best interpreted as a neurovascular canal. This interpretation agrees with the finding of a very large dorsal alveolar canal in AMNH FR 5405, which also must have conducted large vessels along with the maxillary nerve. Taken together, it appears that the nasal cavity and airway had a very rich blood supply.

In summary, CT scanning followed by segmentation and 3D visualization of the nasal systems of some ankylosaurians dramatically changes the assessment of paranasal sinuses in this clade. *Panoplosaurus* and *Euoplocephalus* apparently lacked paranasal sinus diverticula from the respiratory portion of the nasal cavity proper, although they had pneumatic apertures in the palatine bones leading to chambers within the olfactory region. On the other hand, and no less significantly, both taxa were found to have had complex nasal airways, in each case taking a highly convoluted course through the nasal cavity. Although rostral and caudal loops of the airway can be described for both taxa, homology of these loops cannot be assessed until more taxa are sampled. The caudal loops are quite similar, but the rostral loops have some important differences. Comparing the lengths of the airways between the Coombs (1978) models and the new ones proposed here yields some striking differences. For *Panoplosaurus*, the airway reconstructed using a Coombs model is 206 mm, whereas the airway in the new model measures 479 mm—a 232% increase. For *Euoplocephalus*, the Coombs airway is 250 mm, whereas the new airway is 790 mm—a 316% increase. It is worth emphasizing the caveat that the interpretations here are hypotheses based on the authors interpretation of the CT data which, when dealing with fossils, are not always as clear as would be desired. Nevertheless, the symmetry is striking, suggesting that these interpretations are largely correct. Further CT scanning of other specimens, coupled with segmentation and 3D visualization, is necessary to test our novel hypotheses and to assess how widely they pertain. The seemingly contrary finding of a simpler airway in *Edmontonia*—yet still presenting some evidence for internal subdivision (incomplete bony laminae)—raises the question of whether variation in mineralization of nasal structures could make a complicated, convoluted airway appear to be simple.

Head Mass Calculations for *Majungasaurus* and *Tyrannosaurus*

Using the methods described above, mass of the head was calculated for the two theropod dinosaurs in our sample, as well as the human (Tables 1–3). Based on the reconstruction of pneumatic sinuses discussed here

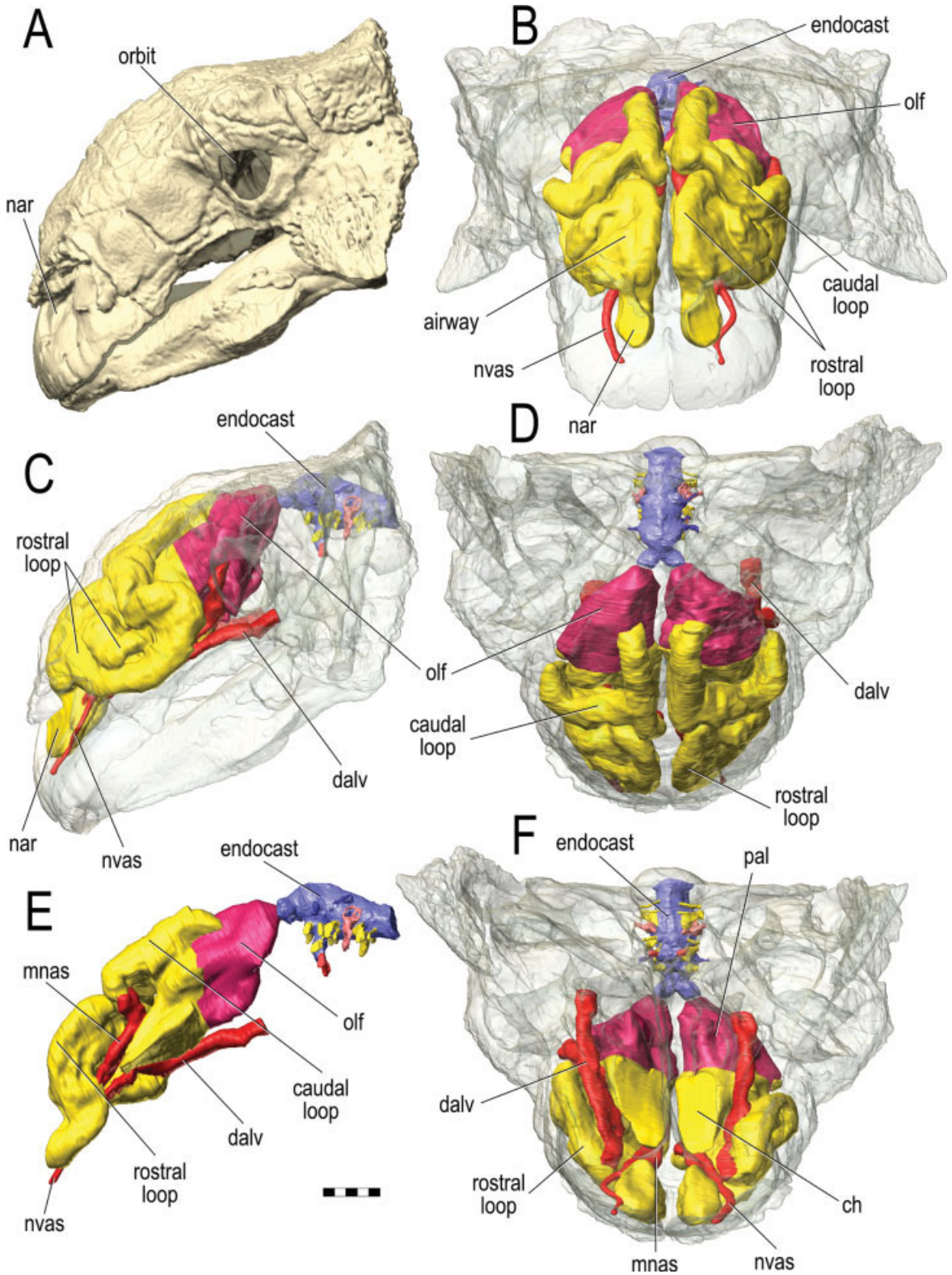

Fig. 8. Paranasal sinuses and other cephalic components of *Euoplocephalus tutus* (AMNH FR 5405) based on CT scanning followed by segmentation and 3D visualization. Bone is rendered semitransparent (except in **A**). **A:** Skull in left lateral view. **B:** Rostral view. **C:** Left lateral view. **D:** Dorsal view. **E:** Right side of sagittally sectioned head in medial view with soft-tissue components isolated. **F:** Ventral view. **G:** Left rostrodorsolateral view. **H:** Isolated and semitransparent nasal cavity in left rostrodorsolateral view, revealing the course of the nasal airway (arrow). **I**: Same in left lateral view. Scale bars = 5 cm.

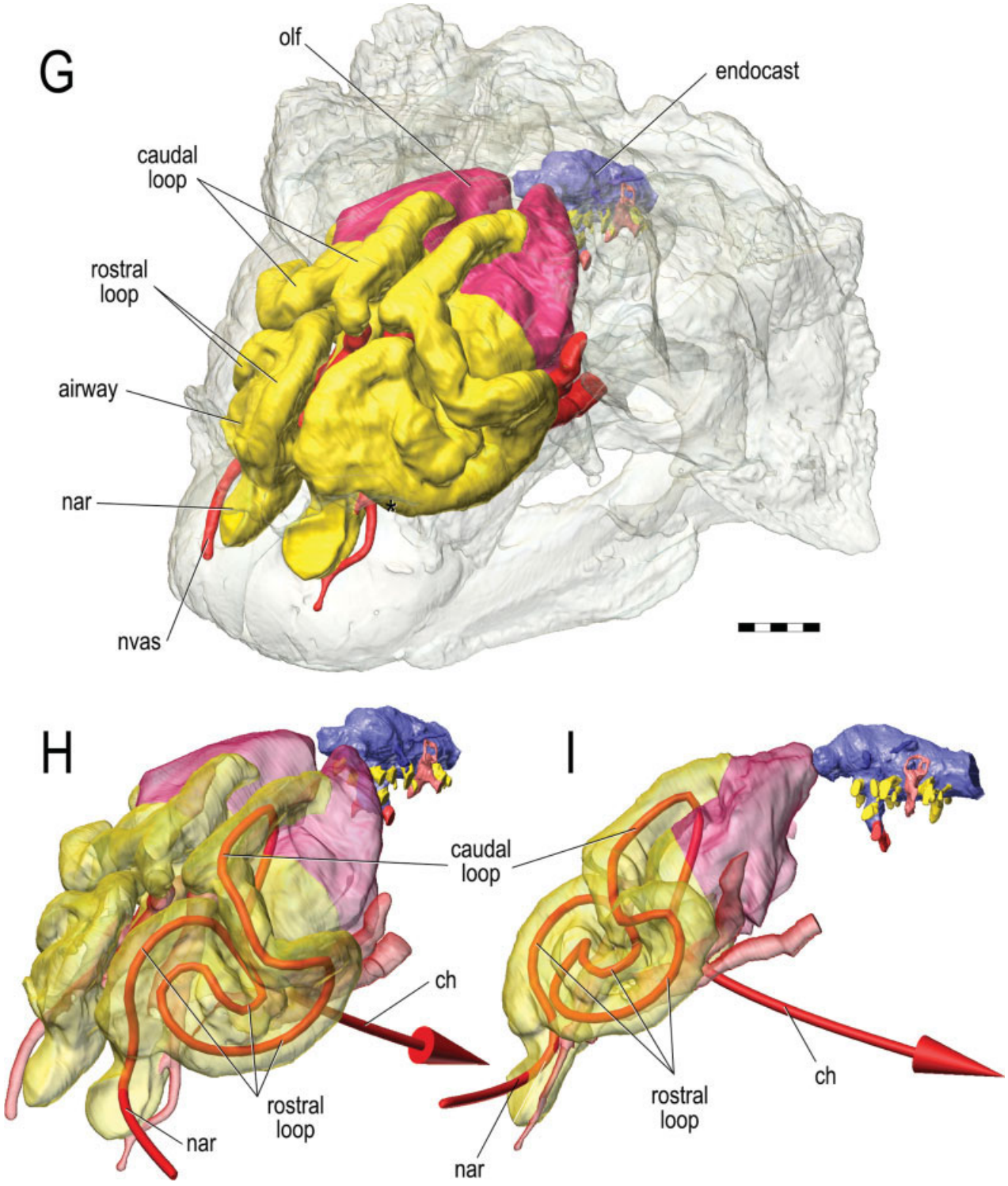

Figure 8. (continued)

(Figs. 5 and 6), the heads of *Majungasaurus* and *Tyrannosaurus* weighed 32.1 and 515.5 kg, respectively. The bony skulls (meaning real bone, not fossilized bone) would have weighed 8.0 and 16.6 kg, respectively. The tables also list the volumes of the various paranasal and paratympanic sinuses. Table 4 presents the results of the calculations comparing the proportion of the head and skull occupied by sinuses. Tables 1–4 also present

TABLE 4. Proportional comparisons of sinus contributions to head and skull volume and mass in *Majungasaurus*, *Tyrannosaurus*, and *Homo*

	Majungasaurus	*Tyrannosaurus*	*Homo*
Paranasal sinus volume[a]/skull volume[b]	0.184	0.131	0.076
Paranasal sinus volume/head volume	0.052	0.054	0.019
Paratympanic sinus volume/skull volume[b]	0.004	0.035	0.018
Paratympanic sinus volume/head volume	0.001	0.010	0.004
Cranial endocast volume/head volume	0.004	0.002	0.453
Skull mass (g) [per cent] savings due to paranasal sinuses[c]	1818.2 [0.185]	26113.2 [0.136]	53.3 [0.077]
Skull mass (g) [per cent] savings due to all pneumaticity[d]	1855.0 [0.189]	33026.4 [0.166]	65.9 [0.094]
Head mass (g) [per cent] savings due to paranasal sinuses[e]	2238.7 [0.065]	36309.3 [0.066]	53.3 [0.020]
Head mass (g) [per cent] savings due to all pneumaticity[f]	2278.5 [0.066]	43222.5 [0.077]	65.9 [0.024]

[a]Paranasal sinus volume excludes the suborbital sinus.
[b]Skull volume includes the volume of intraosseous sinuses.
[c]Calculated as mass of skull with paranasal sinuses[a] converted to bone relative to skull mass with sinuses air-filled.
[d]Calculated as mass of skull with all sinuses converted to bone relative to skull mass with sinuses air-filled.
[e]Calculated as mass of head with paranasal sinuses[a] converted to bone relative to head mass with sinuses air-filled.
[f]Calculated as mass of head with all sinuses converted to bone relative to head mass with sinuses air-filled.

information on the differences in masses for both heads and skulls based on (1) whether the paranasal sinuses are filled with air or bone and (2) whether the paratympanic as well as the paranasal sinuses are filled with bone. These data provide an estimate of the savings in mass due to the presence of air sinuses for these different species. These savings are more explicitly summarized in Table 4 and explored more fully in the discussion.

DISCUSSION

Active Ventilation of Dinosaur Paranasal Air Sinuses

The inferred presence of the suborbital diverticulum in theropod dinosaurs, such as *Majungasaurus* and *Tyrannosaurus*, signals a fundamentally different functional organization of the paranasal sinuses than that observed in mammals. Mammalian paranasal sinuses are dead-air spaces that, with the exception of a typically small ostium connecting the epithelial diverticulum to the nasal cavity proper, are cul-de-sacs more or less fully enclosed within bone. As a result, air moves between the nasal cavity and sinus very slowly and largely by diffusion. In birds, however, such as the ostrich showcased here (Fig. 4), the suborbital sinus extends caudally out of the antorbital cavity and passes into the orbit where it interleaves with a diversity of tissues, most importantly the jaw muscles. Because the suborbital sinus directly contacts these muscles (often insinuating itself between the muscle bellies), the sinus epithelium is affected by the adduction/abduction cycles of the jaws. Positive and negative pressures, respectively, are experienced within the suborbital sinus air space, which then transfers those pressures throughout the system and back to the antorbital sinus ostium where air would flow back and forth. Thus, unlike mammals, the paranasal sinuses of birds and apparently at least some extinct dinosaurs were actively ventilated, with jaw movements acting like a bellows pump to move air through the system (Witmer, 1997a,b, 1999). To date, there have been no *in vivo* experimental studies of this system, although it is readily demonstrated on cadaveric birds, and, anecdotally, the authors have observed the skin overlying the antorbital sinus pulsating in phase with mandibular movements in live domestic turkey. More to the point, there does not appear to be any mechanism that would prevent active ventilation; that is, it seems to be an inherent physical design characteristic of the system, regardless of whether it confers any advantage.

Active ventilation may have been widespread in extinct archosaurs in that many clades have skulls with a general construction that is similar to that of theropods. Again, the suborbital sinus does not routinely pneumatize bone in extant birds or extinct theropods, and so its presence is difficult to infer outside of the few cases where positive evidence exists (e.g., *Majungasaurus*, *Tyrannosaurus*, dromaeosaurids; see also Witmer, 1997a) and those taxa phylogenetically nested between them. It is known that some archosaurs lack this system. The paranasal sinuses of extant crocodilians, for example, are generally mammal-like in being cul-de-sacs. Likewise, the ankylosaurians discussed here could not have had a suborbital sinus because their nasal cavities and antorbital regions are largely walled off from the orbit, and this is true for many other ornithischian dinosaur clades (Witmer, 1997a). And even in those taxa with active sinus ventilation, the intraosseous components (e.g., lacrimal sinuses of theropods, fronto-ethmoid sinuses of birds) would still be cul-de-sacs, the exception being the nasal sinus of *Majungasaurus* which potentially was ventilated via the communication it afforded between the contralateral antorbital sinuses. It is tempting to read biological meaning into these differences between clades in possession of the suborbital sinus and active ventilation, but they could relate more to constraints of skull architecture than sinus function. Moreover, the physiological impact of active ventilation of sinuses is unknown. However, active ventilation opens up the possibility of evaporative cooling, and research in the authors' laboratory reveals a dense vascular network associated with the antorbital and suborbital sinuses in modern birds. Thus, active ventilation could play some role in thermal biology.

Paranasal Sinuses in the Context of Dinosaur Head Anatomy

Paranasal sinuses do not exist in isolation, but rather are integral components of head anatomy. For example, the paranasal sinuses are not just the "spaces between the braces" (DuBrul, 1998, p 49), but actually inflate bones in a number of archosaur taxa such that they are larger than they might be otherwise. Examples include the nasal of *Majungasaurus* and the palatine and maxillary sinuses of *Tyrannosaurus*. In these cases, pneumatization actually increases the mass of the inflated element, because the amount of bone tissue must be increased to enclose the diverticulum. There may be functional or architectural constraints (or selection pressures) dictating a decoupling of internal and external bone form (Witmer, 1997a), and pneumatization may have provided the mechanism to displace bone surfaces. To continue these examples, pneumatic inflation of the nasal of *Majungasaurus* may have been the mechanism to increase the size of a visual display organ. For *Tyrannosaurus*, pneumatic inflation of the maxillary sinuses may have been the mechanism to modify the structure of the respiratory portion of the nasal cavity by constricting the airway such that it passed through the dorsal portion of the snout (perhaps in association with air-streaming dynamics). Likewise, pneumatization provides a mechanism to alter the form and hence the biomechanical properties of bones. For example, pneumatization of the lacrimal bone of *Tyrannosaurus* changes the cross-sections of its rami from being relatively flat (the primitive condition) to being circular and hollow. Although Molnar (2000) argued that the sinuses might weaken the skull of *Tyrannosaurus*, these shape changes would increase the second moment of area and polar moment of inertia and hence enhance bending and torsional rigidity, respectively, which, given the potential bite forces generated by *Tyrannosaurus* (Erickson et al., 1996; Meers, 2002), may have been important. On the other hand, in the case of the palatine sinus of *Tyrannosaurus* or some of the nasopharyngeal duct sinuses of crocodilians, the diverticula appear to have simply expanded because they could (Witmer, 1997a), producing almost grotesque bone shapes that, if anything, would hinder other functions, such as muscle attachment.

Whereas theropod dinosaurs in general show a trend for expansion of the antorbital sinus and its subsidiary diverticula, some clades show a reduction (Witmer, 1997a,b). Our new findings presented here now suggest that ankylosaurian ornithischians, many of which were previously thought to have extensive sinuses, may also have reduced or even lost the antorbital sinus. Both the nodosaurid *Panoplosaurus* and the ankylosaurid *Euoplocephalus* had a dramatically elongate and convoluted nasal airway that expanded into the region normally occupied by the antorbital sinus in other archosaurs. Thus, modifications to airway conformation may be causally linked to reduction and/or loss of paranasal sinuses in at least some ankylosaurs. The apparent variation seen in nasal cavity structure in ankylosaurians may reflect differing amounts of ossification (e.g., some individuals with apparently "simple" airways may not have ossified the cartilaginous capsular structures) or may reflect real differences in anatomical organization, perhaps relating to differences in the physiological functions of the nasal cavity (e.g., thermal phenomena) or even behavioral factors pertaining to vocal resonance.

The paranasal sinuses of many archosaurs are not restricted to the facial skeleton, but also expand into other areas of the head. As in many mammals, paranasal air sinuses sometimes expand into the skull roof and pneumatize the bones of the braincase. In the case of birds (Fig. 4), a novel fronto-ethmoidal sinus evaginates from the nasal cavity proper to extend into the bone above the cerebrum. Alligators uniquely have a sinus in the prefrontal bone that resides directly adjacent to the olfactory bulbs of the brain (Fig. 3). Likewise, *Majungasaurus* had an unusual sinus within the frontal bone that sits directly above the olfactory tracts and bulbs. An interesting difference between archosaurs and mammals is that, whereas pneumaticity of the skull roof and braincase in mammals typically derives from the paranasal sinuses (e.g., sphenoid and frontal), such pneumaticity in archosaurs is relatively rare (the examples just noted) and, instead, the braincase is much more commonly and extensively pneumatized by the paratympanic sinuses (Figs. 5 and 6), which typically are restricted to the mastoid region of the temporal bone in mammals (Fig. 1). In many archosaurs, such as the alligator (Fig. 3), ostrich (Fig. 4), and tyrannosaur (6) described here, the paratympanic air sinuses encircle the bones of the brain cavity. Of course, as discussed in the previous section, the most remarkable attribute of the paranasal sinus systems of at least some archosaurs is the suborbital sinus that interacts with many anatomical systems in the head, ranging from the eyeball and extraocular muscles to the jaw adductor musculature to a variety of neurovascular structures.

Weighing a Dinosaur Head: The Contribution of Sinuses to Total Head Mass

Combining information derived from anatomical dissection of extant archosaurs, detailed study of fossil specimens of extinct archosaurs, and CT scanning of extant and extinct archosaurs alike, a more sophisticated and fine-scale view of cephalic anatomy in dinosaurs and their kin is starting to emerge. One outcome of being able to specify the locations and dimensions of anatomical components within a digital environment is that we can now generate reliable information on volumes of those components, from which masses can be calculated. Tables 1–4 present the volumes and masses of various anatomical components for the theropods *Majungasaurus* and *Tyrannosaurus*. Summing these values, very credible and defensible estimates of head mass, for the first time, can be calculated for an extinct animal. Again, for *Majungasaurus*, head mass was about 32 kg, whereas for *Tyrannosaurus* head mass was about 515 kg. A useful "reality check" is simply to ignore all of our reconstructions of air sinuses and tissue-density estimates and calculate the mass of the "heads" (based on our very conservative "skinning" and the head volumes in Tables 1 and 2) as if they were a homogenous bag of water (density = 1 g/cm^3): 33 kg for *Majungasaurus* and 534 kg for *Tyrannosaurus*. These values are close enough to our reconstructed head masses to confirm that our methods produce credible results. Head masses for extant taxa are difficult to find in the literature, and so the heads of three large mammals that

were on hand were weighed to provide comparison with more familiar animals: giraffe (*Giraffa camelopardalis*, female, OUVC 10513): 20.3 kg; Florida manatee (*Trichechus manatus*, sex unknown, OUVC 10514: 24.4 kg; white rhinoceros (*Ceratotherium simum*, male, OUVC 9754): 115.9 kg. Thus, the head of *Tyrannosaurus* weighed more than four adult male rhino heads.

These new calculations of head mass for the dinosaurs are useful in at least a couple of ways. First, they signal a new level of precision in measuring mass, perhaps the single most important biological parameter, thus holding the prospect of extending such capabilities beyond the head to the rest of the animal. Body mass estimates typically have been very indirect measures, such as regressions of femoral circumference (Anderson et al., 1985) or graphical-computational methods based on life drawings or outlines (Henderson, 1999; Seebacher, 2001). Accurate soft-tissue reconstruction within the body, coupled with digital analysis and volumetric calculations, may allow for more precise, defensible, and testable estimates of body mass. The approaches presented here are still in their infancy, but the fact that almost every step is a testable hypothesis is an advance. Second, these data on head masses are immediately useful for functional studies that draw on head movements or movements of the whole body. For example, there are a series of papers on the turning capabilities in theropods that discuss the role of the large cantilevered head in theropods and its impact on rotational inertia—head mass is a key parameter (Carrier et al., 2001; Henderson and Snively, 2003). Likewise, in Snively and Russell's (2007b) excellent recent analysis of cervicocephalic function in *Tyrannosaurus*, the authors, of necessity, had to do a very rough sensitivity analysis to account for the air sinuses, running separate analyses with density assigned to that of water (1 g/cm^3), air (0 g/cm^3), and arbitrarily halfway between the two (0.5 g/cm^3). In fact, they noted (Snively and Russell, 2007b, p 632), "Variation in antorbital density has a potentially greater effect. . ., with rotational inertia of the head increasing by 20% if the antorbital space had a specific gravity of 1 versus that of air." Thus, precise knowledge of head mass has bearing on a range of functional hypotheses.

Beyond head mass itself, the contribution of the paranasal sinuses to the volume and mass of both the head and the skull (Table 4) can be explored. Volumetrically, the paranasal sinuses in the theropods comprise a considerable proportion of skull volume (13%–18%), more so than in humans (8%). However, when measured relative to head volume, the numbers drop: 5% for the theropods and 2% for humans. The paratympanic sinuses make up a trifling proportion of head volume in any of the sample, peaking at 1% in *Tyrannosaurus*, and indeed even for skulls, the paratympanic sinuses comprise less than 5% of skull volume for the theropods and human alike. Turning to masses, an interesting experiment is to turn air to bone by assigning the volumes of the intraosseous sinuses the density of bone, allowing some measure of how much weight is saved by the presence of pneumatic sinuses. A quick caveat, as noted above, is that this comparison is not entirely fair in that pneumatic inflation increases bone dimensions (e.g., nasal sinus of *Majungasaurus*, maxillary and palatine sinuses of *Tyrannosaurus*) beyond what they would be in an apneumatic state. Nevertheless, the experiment is illustrative. The mass savings for the skull provided by the paranasal air sinuses are large for both theropods (14%–18%), and the savings increase about another 3% for *Tyrannosaurus* when its extensive paratympanic sinuses are also considered. As with volumes, the mass savings become much less dramatic when considered for the whole head and not just the bony skull. An additional factor here is that the air in the suborbital sinuses becomes soft tissue. In this case, the savings provided by the paranasal sinuses drops to about 6.5% for the theropods, rising to near 8% when the paratympanic sinuses of *Tyrannosaurus* are also "filled" with bone. In humans, the same pattern is shown (more savings for the skull, less for the head), but the magnitudes are much smaller, largely because of the enormous human brain (occupying 45% of head volume) in comparison with the famously tiny brains of the dinosaurs (much less than 1% of head volume in both cases).

As discussed in Witmer's (1997a) review of the debates on sinus function, weight reduction or saving has been a surprisingly uncommon suggestion. Quantifying mass savings also had been difficult until now. Savings of 6%–8% of head volume is not particularly impressive, and, as Negus (1958) vigorously argued, it would seem that the neck of most animals is well equipped to cantilever the head. Certainly, Snively and Russell (2007a,b) documented a prodigious cervicocephalic musculature for theropods. A valid question, however, is whether the considerably greater savings in skull mass (up to 18%) was biologically important. In other words, whereas the metabolic costs of carrying around a sinus-less head may be modest, the metabolic costs of maintaining the bone tissue of the skull (up to 33 kg of bone in an apneumatic *Tyrannosaurus*) might be important. Still, given the other evidence suggesting that sinuses, particularly in theropods, are largely and inherently opportunistic and invasive structures (Witmer, 1997a,b, 1999), further evidence is needed to test hypotheses on sinus function and the relative role of mass savings.

ACKNOWLEDGMENTS

The authors thank Samuel Marquéz and Jeffery Laitman for their invitation to participate in this volume. For access to and loan of fossil specimens, they thank M. Lamanna and A. Henrici (Carnegie Museum, Pittsburgh), M. Norell and C. Mehling (AMNH, New York City), P. Makovicky and W. Simpson (FMNH, Chicago), D. Krause (Stony Brook University, Long Island), and D. Evans and K. Seymour (ROM, Toronto). For providing the specimen of *Alligator mississippiensis*, the authors thank R. Elsey, Rockefeller Wildlife Refuge, Grand Chenier, LA. The authors have benefited from discussions with many colleagues at many institutions, including in particular C. Brochu, K. Carpenter, T. Carr, P. Currie, D. Dufeau, D. Evans, G. Erickson, R. Hill, C. Holliday, J. Hutchinson, S. Sampson, J. Sedlmayr, T. Tsuihiji, M. Vickaryous, and D. Weishampel. For help with CT scanning, they thank H. Rockhold, RT (O'Bleness Memorial Hospital, Athens, Ohio) and R. Beshears (NASA Marshall Space Flight Center, Huntsville, Alabama). Witmer Lab members J. Daniel, D. Dufeau, M. Graham, T. Hieronymus, W. Porter, J. Tickhill, and T. Tsuihiji helped in many different ways. M. Vickaryous (University of Calgary, Alberta) provided his unpublished ankylosaur CT

data. B. Cooley (Calgary, Alberta) loaned the authors his sculpture of FMNH PR2081 and permitted it to be CT scanned.

LITERATURE CITED

Anderson JF, Hall-Martin A, Russell DA. 1985. Long bone circumference and weight in mammals, birds, and dinosaurs. J Zool A 207:53–61.

Bang BG, Wenzel BM. 1985. Nasal cavity and olfactory system. In: King AS, McLelland J, editors. Form and function in birds. Vol. 3. New York: Academic Press. p 195–225.

Bininda-Emonds ORP, Cardillo M, Jones KE, MacPhee RDE, Beck RMD, Grenyer R, Price SA, Vos RA, Gittleman JL, Purvis A. 2007. The delayed rise of present-day mammals. Nature 446:507–512.

Brochu CA. 2003. Osteology of *Tyrannosaurus rex*: insights from a nearly complete skeleton and high-resolution computed tomographic analysis of the skull. Soc Vert Paleontol Mem 7, J Vert Paleontol 22 (Suppl 4):1–140.

Brown B. 1908. The Ankylosauridae, a new family of armored dinosaurs from the upper cretaceous. Bull Am Mus Nat Hist 24:187–201.

Carpenter K. 1990. Ankylosaur systematics: example using *Panoplosaurus* and *Edmontonia* (Ankylosauria: Nodosauridae). In: Carpenter K, Currie PJ, editors. Dinosaur systematics: approaches and perspectives. New York: Cambridge University Press. p 281–298.

Carrier DR, Walter RM, Lee DV. 2001. Influence of rotational inertia on turning performance of theropod dinosaurs: clues from humans with increased rotational inertia. J Exp Biol 204:3917–3926.

Coombs WP, Jr. 1978. The families of the ornithischian dinosaur order Ankylosauria. Palaeontology 21:143–170.

Coombs WP, Jr., Maryańska T. 1990. Ankylosauria. In: Weishampel DB, Dodson P, Osmólska H, editors. The Dinosauria. Berkeley: University of California Press. p 456–483.

Currey J. 1984. The mechanical adaptations of bones. Princeton: Princeton University Press.

DuBrul EL. 1988. Sicher and DuBrul's oral anatomy. 8th ed. St. Louis: Ishiyaku EuroAmerica.

Erickson GM, van Kirk SD, Su J, Levenston ME, Caler WE, Carter DR. 1996. Bite-force estimation for *Tyrannosaurus rex* from tooth-marked bones. Nature 382:706–708.

Evans HE. 1996. Anatomy of the budgerigar and other birds. In: Rosskopf WJ, Jr., Woerpel RW, editors. Diseases of cage and aviary birds. 3rd ed. Baltimore: Williams & Wilkins. p 79–162.

Henderson DM. 1999. Estimating the masses and centers of mass of extinct animals by 3-D mathematical slicing. Paleobiology 25:88–106.

Henderson DM, Snively E. 2003. Tyrannosaurus en pointe: allometry minimized rotational inertia of large carnivorous dinosaurs. Proc R Soc B Biol Lett 271:S57–S60.

Hill RV, Witmer LM, Norell MA. 2003. A new specimen of *Pinacosaurus grangeri* (Dinosauria: Ornithischia) from the late Cretaceous of Mongolia: ontogeny and phylogeny of ankylosaurs. Am Mus Novit 3395:1–29.

Holliday CM. 2006. Evolution and function of the jaw musculature and adductor chamber of archosaurs (crocodilians, dinosaurs, and birds). PhD dissertation. Athens, OH: Ohio University.

Holliday CM, Witmer LM. 2007. Archosaur adductor chamber evolution: integration of musculoskeletal and topological criteria in jaw muscle homology. J Morphol 268:457–484.

Holtz TR, Jr., Molnar RE, Currie PJ. 2004. Basal tetanurae. In: Weishampel DB, Dodson P, Osmólska H, editors. The Dinosauria. 2nd ed. Berkeley: University of California Press. p 71–110.

Kilbourne B, Carpenter K. 2005. Redescription of *Gargoyleosaurus parkpinorum*, a polacanthid ankylosaur from the upper jurassic of Albany county, wyoming. Neues Jb Geol Paläontol Abh 237:111–160.

Koppe T, Nagai H, Alt KW. 1999. The paranasal sinuses of higher primates: development, function, and evolution. Chicago: Quintessence.

Krause DW, Sampson SD, Carrano MT, O'Connor PM. 2007. Overview of the history of discovery, taxonomy, phylogeny, and biogeography of *Majungasaurus crenatissimus* (Theropoda: Abelisauridae) from the late cretaceous of Madagascar. Soc Vert Paleontol Mem 8, J Vert Paleontol 27 (Suppl 2):1–20.

Livezey BC, Zusi RL. 2007. Higher-order phylogeny of modern birds (Theropoda, Aves: Neornithes) based on comparative anatomy. II. Analysis and discussion. Zool J Linn Soc 149:1–95.

Maryańska T. 1977. Ankylosauridae (Dinosauria) from Mongolia. Palaeontol Pol 37:85–151.

Meers MB. 2002. Maximum bite force and prey size of *Tyrannosaurus rex* and their relationship to the inference of feeding behaviour. Hist Biol 16:1–12.

Molnar RE. 1991. The cranial morphology of *Tyrannosaurus rex*. Palaeontograph Abteilung A 217:137–176.

Molnar RE. 2000. Mechanical factors in the design of the skull of *Tyrannosaurus rex* (Osborn 1905). Gaia 15:193–218.

Negus VE. 1958. The comparative anatomy and physiology of the nose and paranasal sinuses. London: Livingstone.

Russell LS. 1940. *Edmontonia rugosidens* (Gilmore), an armored dinosaur from the belly river series of Alberta. Univ Toronto Stud Geol 43:3–28.

Ryan MJ, Evans DC. 2005. Ornithischian dinosaurs. In: Currie PJ, Koppelhus EB, editors. Dinosaur provincial park: a spectacular ancient ecosystem revealed. Indianapolis: Indiana University Press. p 312–348.

Sampson SD, Witmer LM. 2007. Craniofacial anatomy of *Majungasaurus crenatissimus* (Theropoda: Abelisauridae) from the late cretaceous of Madagascar. Soc Vert Paleontol Mem 8, J Vert Paleontol 27 (Suppl 2):32–102.

Sanders RK, Smith DK. 2005. The endocranium of the theropod dinosaur *Ceratosaurus* studied with computed tomography. Acta Palaeontol Pol 50:601–616.

Seebacher F. 2001. A new method to calculate allometric length-mass relationships of dinosaurs. J Vert Paleontol 21:51–60.

Sereno PC, Wilson JA, Witmer LM, Whitlock JA, Maga A, Ide O, Rowe TA. 2007. Structural extremes in a Cretaceous dinosaur. PLoS ONE 2:e1230. DOI:10.1371/journal.pone.0001230.

Snively E, Russell AP. 2007a. Functional variation of neck muscles and their relation to feeding style in Tyrannosauridae and other large theropod dinosaurs. Anat Rec 290:934–957.

Snively E, Russell AP. 2007b. Craniocervical feeding dynamics in *Tyrannosaurus rex*. Paleobiology 33:610–638.

Tumanova TA. 1987. The armored dinosaurs of Mongolia [in Russian; Griffith R, translator]. Trans Jt Sov-Mongol Paleontol Exped 32:1–76.

Urbanchek MG, Picken EB, Kalliainen LK, Kuzon WM, Jr. 2001. Specific force deficit in skeletal muscles of old rats is partially explained by the existence of denervated muscle fibers. J Gerontol A 56A:B191–B197.

Vickaryous MK. 2006. New information on the cranial anatomy of *Edmontonia rugosidens* Gilmore, a late cretaceous nodosaurid dinosaur from dinosaur provincial park, Alberta. J Vert Paleontol 26:1011–1013.

Vickaryous MK, Maryańska T, Weishampel DB. 2004. Ankylosauria. In: Weishampel DB, Dodson P, Osmólska H, editors. The Dinosauria. 2nd ed. Berkeley: University of California Press. p 363–392.

Vickaryous MK, Russell AP. 2003. A redescription of the skull of *Euoplocephalus tutus* (Archosauria: Ornithischia): a foundation for comparative and systematic studies of ankylosaurian dinosaurs. Zool J Linn Soc 137:157–186.

Wegner RN. 1958. Die Nebenhöhlen der Nase bei den Krokodilen. Wissensch Z Ernst Moritz Arndt Univ Greifswald 7:1–39.

Witmer LM. 1990. The craniofacial air sac system of Mesozoic birds (Aves). Zool J Linn Soc 100:327–378.

Witmer LM. 1995a. The extant phylogenetic bracket and the importance of reconstructing soft tissues in fossils. In: Thomason JJ, editor. Functional morphology in vertebrate paleontology. New York: Cambridge University Press. p 19–33.

Witmer LM. 1995b. Homology of facial structures in extant archosaurs (birds and crocodilians), with special reference to paranasal pneumaticity and nasal conchae. J Morphol 225:269–327.

Witmer LM. 1997a. The evolution of the antorbital cavity of archosaurs: a study in soft-tissue reconstruction in the fossil record

with an analysis of the function of pneumaticity. Soc Vert Paleontol Mem 3, J Vert Paleontol 17 (Suppl 1):1–73.

Witmer LM. 1997b. Craniofacial air sinus systems. In: Currie PJ, Padian K, editors. The encyclopedia of dinosaurs. New York: Academic Press. p 151–159.

Witmer LM. 1999. The phylogenetic history of paranasal air sinuses. In: Koppe T, Nagai H, Alt KW, editors. The paranasal sinuses of higher primates: development, function and evolution. Chicago: Quintessence. p 21–34.

Witmer LM, Chatterjee S, Franzosa J, Rowe T. 2003. Neuroanatomy of flying reptiles and implications for flight, posture and behaviour. Nature 425:950–953.

Witmer LM, Ridgely RC. 2005. Tyrannosaur brain and ear structure: ontogeny and implications for sensory function and behavior. J Vert Paleontol 25 (Suppl 3):131A.

Witmer LM, Ridgely RC. The Cleveland tyrannosaur skull (*Nanotyrannus* or *Tyrannosaurus*): new findings based on CT scanning, with special reference to the braincase. Kirtlandia, in press.

Witmer LM, Ridgely RC, Dufeau DL, Semones MC. 2008. Using CT to peer into the past: 3D visualization of the brain and ear regions of birds, crocodiles, and nonavian dinosaurs. In: Endo H, Frey R, editors. Anatomical imaging: towards a new morphology. Tokyo: Springer-Verlag. p 67–87.

Witmer LM, Ridgely RC, Sampson SD. 2004. The ear region, cerebral endocast, and cephalic sinuses of the abelisaurid theropod dinosaur *Majungatholus*. J Vert Paleontol 24 (Suppl 3):131A.

Yang J, Chiou R, Ruprecht A, Vicario J, MacPhail LA, Rams TE. 2002. A new device for measuring density of jaw bones. Dentomaxillofac Radiol 31:313–316.